Mathematisches Forschungsinstitut Oberwolfach

Report No. 13/2015

DOI: 10.4171/OWR/2015/13

Discrete Differential Geometry

Organised by
Alexander I. Bobenko, Berlin
Richard Kenyon, Providence
Peter Schröder, Pasadena

1 March – 7 March 2015

Abstract. This is the collection of extended abstracts for the 26 lectures and the open problem session at the fourth Oberwolfach workshop on Discrete Differential Geometry.

Mathematics Subject Classification (2010): 52Cxx, 53xx, 57xx, 68U05.

Introduction by the Organisers

Discrete Differential Geometry is a very productive research area on the border between differential and discrete geometry. It aims to develop discrete equivalents of various notions and methods from classical differential geometry. The focus on discretization problems ensures strong connections to mathematical physics, numerical analysis, computer graphics and other applications.

This was the fourth Discrete Differential Geometry conference at Oberwolfach. The subject has evolved significantly since its beginning a decade ago. This years's conference higlighted advances in particular in the areas of discrete uniformization, discrete surface theory, mathematical structures of integrability and cluster algebras, discretizations of PDEs and analysis on manifolds with applications to computer graphics.

The workshop featured many talks on discrete differential geometry problems motivated by applications in computer graphics. This area becomes an increasingly important source of inspiration for theoretical advances in discrete differential geometry. Some systems have natural discretizations which have even more mathematical structure then their continuous counterparts, and often finding the right discretizations makes a huge difference in efficiency. This phenomenon was demonstrated in many talks. The variety of problems varied from new ideas on generating of strip patterns with constant spacing in the talk by Pinkall, and on modelling of (piecewise) developable surfaces in the talk by Wallner to a representation of discrete vector fields as linear operators by Ben-Chen. Further topics directly related to applications included spectral analysis on meshes (Tong), seamless mappings between meshes (Lipman), linear operators on surfaces of revolution (Kazhdan), surfaces with nested layers (Jacobson), topological data analysis of shapes from sampled data (Bauer), consequent optimization with various norms (Zorin).

Traditionally for this workshop new results on discrete uniformization theory were presented. This includes a new uniformization theorem of surfaces with polyherdal metric (Luo), dealing with meshes with changing combinatorics. Discrete conformal maps for general polyhedral surfaces and in particular experimental results on their convergence to smooth conformal maps were discussed by Springborn. Other talks on harmonicity (discrete enharmonic functions) and holomorphicity (discrete s-holomorphic functions appearing in the Ising model) were due to Kenyon and Chelkak. A description of inscribed polytopes related to discrete uniformization theory was given by Schlenker. Sanyal developed a quite different side of the polytope theory based on convex algebraic geometry.

Discrete surface theory is another traditional topic at this workshop. This year there was an emphasis on merging of the methods from the general theory of simplicial surfaces and from integrable geometry: We had talks on simplicial (non-parametrized) special classes of surfaces (Lam) as well as on quadrilateral (parametrized) rather general surfaces (Sageman-Furnas). Rörig described a piecewise smooth extension of nets with planar quadrilateral faces. A completely different approach of modelling surfaces as origami tesselations was presented by Vouga.

Mathematical structures of integrability and cluster algebras was another hot topic of the workshop. Here we heard talks by Schief, King and Fock on distinguished discrete integrable models as well as on various approaches aiming at their classification.

A solution of a classification problem coming from Riemannian geometry was presented in the talk by Brehm. There were also a few talks (Akopyan, Nilov, Tabachnikov) on concrete geometric problems including line nets with circumscribed quadrilaterals, circular webs and the circumcenter of mass.

The organizers are grateful to all participants for all the lectures, discussions, and conversations that combined into this very lively and successful workshop - and to everyone at Research Institute in Oberwolfach for the perfect setting.

Acknowledgement: The MFO and the workshop organizers would like to thank the National Science Foundation for supporting the participation of junior researchers in the workshop by the grant DMS-1049268, “US Junior Oberwolfach Fellows”.

Workshop: Discrete Differential Geometry

Table of Contents

Abstracts

Some small theorems about discrete conformal maps

Boris Springborn
(joint work with A. Bobenko, S. Sechelmann, U. Bücking, and S. Born)

We consider polyhedral surfaces made from gluing convex euclidean polygons that are inscribed in circles. Two such surfaces are considered *discretely conformally equivalent* if they are combinatorially equivalent and the lengths ℓ_{ij} and $\tilde{\ell}_{ij}$ of corresponding edges are related by $\tilde{\ell}_{ij} = e^{\frac{u_i+u_j}{2}}\ell_{ij}$, where u_i are logarithmic scale factors associated to the vertices. For triangulations, inscribability of faces is no restriction and this notion of discrete conformal equivalence is well known [4], [3].

The first part of the talk is concerned with observations and results [2] about the similarities and differences of discrete conformal equivalence for triangulations and for general polyhedral surfaces, in particular if all face degrees are even, or equal to four. Two triangulations are discretely conformally equivalent if and only if the *length cross ratios* for corresponding interior edges are equal [3]. Two quadrangulations are discretely conformally equivalent, if and only if the complex cross ratios of corresponding faces are equal. Like in the triangle case, the discrete conformal mapping problem (find a discretely conformally equivalent surface with prescribed angle sums at vertices) is variational: The unknown logarithmic scale factors minimize a convex functional. This implies that solutions are unique if they exist. We comment on a couple of phenomena that are particular to quadrangulations and connected to the the edge graph being bipartite: the occurrence of orthogonal circle patterns among the solutions, and necessary conditions on angle sums at the boundary that have to hold for "black" and "white" vertices separately. We discuss examples of discrete conformal maps and experimental results on the rate of convergence to smooth conformal maps (which is conjectured).

The second part of the talk, which had to be cut due to lack of time, was to deal with results on the quasiconformal distortion of projective maps and applications to discrete conformality [1]. The starting point of this research was the observation that *circumcircle preserving piecewise projective interpolation* between triangulations, which is continuous across the edges if and only if two triangulations are discretely conformally equivalent, "looks better" than piecewise linear interpolation [5]. Is this due to lower quasiconformal distortion? As it turns out, the contour lines of the quasiconformal distortion of a projective transformation of $\mathbb{RP}^2$ (that is not an affine transformation) form a hyperbolic pencil of circles. (We identify $\mathbb{RP}^2$ with the union of $\mathbb{C}$ and a line at infinity.) The circles of this pencil are the only circles that are mapped to circles. When a triangle is mapped to another triangle by a circumcircle preserving projective transformation, the maximal quasiconformal distortion is attained simultaneously at all three vertices, and this value is equal to the constant quasiconformal distortion of the affine linear map between the triangles. Of all projective transformations that map between two fixed triangles, the maximal quasiconformal distortion is minimal for the projective transformation that maps angle bisectors to angle bisectors. *Angle bisector preserving piecewise projective interpolation* is also continuous across edges if and only if the triangulations are discretely conformally equivalent. There is a one-parameter family of piecewise projective interpolations with this property, of which the circumcircle and angle bisector preserving ones are special cases.

References

[1] U. Bücking, S. Born B. Springborn, *Quasiconformal distortion of projective maps*, in preparation.

[2] A. Bobenko, S. Sechelmann, B. Springborn, *Discrete uniformization of Riemann surfaces*, in preparation.

[3] A. Bobenko, U. Pinkall, B. Springborn, *Discrete conformal maps and ideal hyperbolic polyhedra*, arXiv:1005.2698, to appear in Geometry & Topology.

[4] F. Luo, *Combinatorial Yamabe flow on surfaces*, Commun. Contemp. Math. 6 (2004), no. 5, 765–780.

[5] B. Springborn, P. Schröder, and U. Pinkall, *Conformal equivalence of triangle meshes*, in ACM SIGGRAPH 2008 papers (SIGGRAPH '08), ACM, New York, 2008, article 77, 11 pages.

From isothermic triangulated surfaces to discrete holomorphicity

Wai Yeung Lam

(joint work with Ulrich Pinkall)

Isothermic surfaces are building blocks in classical differential geometry. They include all surfaces of revolution, quadrics, constant mean curvature surfaces and many other interesting surfaces. A smooth surface in Euclidean space is called isothermic if it admits conformal curvature line parametrization around every point. However there are various characterizations of isothermic surfaces that do not refer to special parametrizations.

We propose a definition of isothermic triangulated surfaces which does not involve the notion of conformal curvature line parametrizations. Its motivation is a result from the smooth theory that a surface is isothermic if and only if locally it admits an infinitesimal isometric deformation preserving the mean curvature. Let V_{in}, E_{in} denote the sets of interior vertices and edges respectively.

Definition 1. A triangulated surface $f : M \to \mathbb{R}^3$ is *isothermic* if there exists a $\mathbb{R}^3$-valued dual 1-form τ such that

$$\sum_j \tau(*e_{ij}) = 0 \quad \forall v_i \in V_{in}$$

$$df(e) \times \tau(*e) = 0 \quad \forall e \in E_{in}$$

$$\sum_j \langle df(e_{ij}), \tau(*e_{ij}) \rangle = 0 \quad \forall v_i \in V_{in}.$$

Corollary 1. *A simply connected triangulated surface immersed in Euclidean space is* isothermic *if and only if there exists a non-trivial infinitesimal isometric deformation preserving the integrated mean curvature $H : V_{in} \to \mathbb{R}$ defined by*

$$H_i := \sum_j \alpha_{ij} \ell_{ij} \quad \forall v_i \in V_{in}$$

where α and ℓ denote dihedral angles and edge lengths respectively.

These triangulated surfaces resemble isothermic surfaces in the smooth theory. Isothermic triangulated surfaces can be characterized in terms of the theory of discrete conformality: circle patterns and conformal equivalence. It is shown that this definition generalizes isothermic quadrilateral meshes proposed by Bobenko and Pinkall. In particular,

Theorem 1. *The class of isothermic triangulated surfaces is Möbius invariant.*

As a result, we obtain a discrete analogue of the Weierstrass representation for minimal surfaces. We define discrete minimal surfaces as the reciprocal-parallel meshes of triangulated surfaces with vertices on a sphere. The Weierstrass data consists of an immersed planar triangular mesh and a discrete harmonic function. Given an immersed planar triangular mesh, there is a 1-1 correspondence between discrete harmonic functions and the reciprocal-parallel meshes of its spherical image. Such harmonic functions appear in linear discrete complex analysis with applications to statistical physics (see Smirnov [5]). Figure 1 shows that our construction can be applied to minimal surfaces with umbilic points.

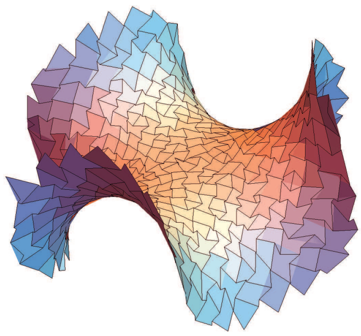

Figure 1. A discrete minimal surface with an umbilic point

Finally, we focus on planar triangular meshes. A simple relation among conformal equivalence, circle patterns and the linear theory of discrete complex analysis is found [3].

References

[1] A. I. Bobenko, C. Mercat, and Y. B. Suris, *Linear and nonlinear theories of discrete analytic functions. Integrable structure and isomonodromic Green's function.* J. Reine Angew. Math. **583**, 117–161 (2005).

[2] A. Bobenko, U. Pinkall, Discrete isothermic surfaces, J. Reine Angew. Math. **475**, 187–208 (1996).
[3] W.Y. Lam, U. Pinkall, *Infinitesimal deformations of triangle meshes and discrete holomorphicity*, In preparation.
[4] W.Y. Lam, U. Pinkall, *Isothermic triangulated surfaces*, preprint (2015), arXiv:1501.02587.
[5] S. Smirnov, *Discrete complex analysis and probability*, Proceedings of the International Congress of Mathematicians. Volume I, pages 595–621. Hindustan Book Agency, New Delhi, 2010.

Towards a curvature theory for general quad meshes

Andrew O. Sageman-Furnas
(joint work with Tim Hoffmann and Max Wardetzky)

Motivation from integrable geometry

Surfaces of constant (mean or Gauss) curvature are often expressed in special parametrizations (e.g., conformal curvature line or asymptotic line), where their integrability equations reduce to completely integrable ("soliton") PDEs from theoretical physics. For each of these specially parametrized constant curvature surfaces, there exists a one parameter *associated family* that stays within the surface class (e.g., minimal surfaces stay minimal), but the parametrization may change.

Discrete partial finite difference analogues for many of these integrable PDEs have been discovered, where discrete integrability is encoded by a certain closing condition around a 3D cube [5]. In this way algebraic constructions for discrete analogues of different classes of surfaces (reviewed in [3]), such as minimal surfaces, surfaces of constant mean curvature, and constant negative Gauss curvature, have been described, together with their one parameter associated families. However, a general notion of curvatures for these surfaces that is constant for the appropriate algebraic constructions has been lacking.

Investigating the geometry of these algebraic families leads us to the following curvature theory, which not only retrieves the thoroughly investigated curvature definitions in the case of planar quads [8, 4], but extends to the general setting of nonplanar quad meshes.

Quad meshes as discrete parametrized surfaces

A natural discrete analogue of a smooth parametrized surface patch is given by a *quad mesh patch*, a map $f : D \subset \mathbb{Z}^2 \to \mathbb{R}^3$ with nonvanishing straight edges. Notice, in particular, that the quadrilateral faces in $\mathbb{R}^3$ may be *nonplanar*. Piecing together such patches defines a *quad mesh* with more general combinatorics and is understood as an atlas for a surface. To every vertex of a quad mesh we associate a unit "normal" vector and define the corresponding map, written per patch as $n : D \subset \mathbb{Z}^2 \to \mathbb{S}^2$, as the *discrete Gauss map*. An arbitrary Gauss map will not be "normal" to its quad mesh, so we only allow for those Gauss maps that satisfy a certain constraint along each edge. The resulting class of *edge-constraint quad meshes* is our focus.[1]

Definition 1. A quad mesh f with Gauss map n is called *edge-constraint* if for every edge of f in $\mathbb{R}^3$ the average of the normals at its end points is perpendicular to f, i.e., for $i = 1, 2$ we have $(f_i - f) \cdot \frac{1}{2}(n_i + n) = 0$.

Curvatures from offsets. For an edge-constraint quad mesh f with Gauss map n, the *offset family* is given by adding multiples of the Gauss map to each vertex, i.e., $f^t := f + tn$. Notice that every mesh of the offset family is edge-constraint with the same Gauss map. In the smooth setting, corresponding tangent planes between a surface, its normal offsets, and common Gauss map are parallel. This allows one to compare areas and derive curvatures.

In order to mimic this definition of curvatures in the discrete case, let $Q_n = (n, n_1, n_{12}, n_2)$ be a Gauss map quad with corresponding quad $Q_f = (f, f_1, f_{12}, f_2)$ and offset quads Q_{f^t}. Define the *discrete Gauss map partial derivatives* as the midpoint connectors of Q_n, i.e., $n_x := \frac{1}{2}(n_{12} + n_1) - \frac{1}{2}(n_2 + n)$ and $n_y := \frac{1}{2}(n_{12} + n_2) - \frac{1}{2}(n_1 + n)$. We define the *common quad tangent plane* between Q_n, Q_f, and Q_{f^t} as the plane spanned by n_x, n_y; and we call $N := \frac{n_x \times n_y}{\|n_x \times n_y\|}$ the *projection direction*.[2] The midpoint connectors of Q_f and Q_{f^t} do not lie in this common tangent plane, so we project them to the plane spanned by n_x and n_y. The partial derivatives f_x, f_y and f^t_x, f^t_y are each defined as the projection (induced by N) of the corresponding midpoint connectors.

The curvature theory for edge-constraint quad meshes is now built per quad and mimics the smooth setting.

Definition 2. The *mixed area form* per quad of two quad meshes g, h sharing a Gauss map n is given by $A(g, h) := \frac{1}{2}(\det(g_x, h_y, N) + \det(h_x, g_y, N))$.

Note that when corresponding quads of g, h and n are in fact planar, lying in parallel planes, and $h = g$ then the quantity $A(g, g)$ coincides with the usual area of a quad.

Lemma 1. *The area of an offset quad satisfies the* Steiner formula*:* $A(f^t, f^t) = A(f, f) + 2tA(f, n) + t^2 A(n, n)$.

As in the smooth setting, factoring out $A(f, f)$ defines the mean and Gauss curvature.

Definition 3. The mean and Gauss curvature per quad of an edge-constraint quad mesh are given by $\mathcal{H} := \frac{A(f,n)}{A(f,f)}$ and $\mathcal{K} := \frac{A(n,n)}{A(f,f)}$, respectively.

[1] We make use of *shift notation* to describe quantities per quad: $f := f(k, \ell), f_1 := f(k+1, \ell)$, and $f_2 := f(k, \ell + 1)$, so $f_{12} := f(k + 1, \ell + 1)$; n, n_1, n_2, and n_{12} are defined similarly.

[2] To include the cases when n_x and n_y are parallel (corresponding to *developable*, i.e., vanishing Gauss curvature, surfaces), we in fact define a *family of projection directions* $U := \{N \in \mathbb{S}^2 | \ N \perp \operatorname{span}\{n_x, n_y\}\}$. The mean and Gauss curvatures are invariant to the choice of $N \in U$.

Fundamental forms, shape operator, and principal curvatures. Fundamental forms of a parametrized surface can be written in terms of the partial derivatives in the tangent plane at each point. The same formulas define these objects per common quad tangent plane of an edge-constraint quad mesh.

Definition 4. The *fundamental forms* are defined as $\mathrm{I} := \begin{pmatrix} f_x \cdot f_x & f_x \cdot f_y \\ f_y \cdot f_x & f_y \cdot f_y \end{pmatrix}$, $\mathrm{II} := \begin{pmatrix} f_x \cdot n_x & f_x \cdot n_y \\ f_y \cdot n_x & f_y \cdot n_y \end{pmatrix}$, and $\mathrm{III} := \begin{pmatrix} n_x \cdot n_x & n_x \cdot n_y \\ n_y \cdot n_x & n_y \cdot n_y \end{pmatrix}$. The shape operator is given by $\mathrm{S} := \mathrm{I}^{-1}\mathrm{II}$.

Observe that the Gauss map being normal to the surface guarantees the existence of principal curvatures and curvature lines.

Lemma 2. *The edge-constraint implies that the second fundamental form is symmetric* ($f_x \cdot n_y = n_x \cdot f_y$)*, so the shape operator is diagonalizable.*

Definition 5. The real eigenvalues k_1, k_2 of the shape operator are the *principal curvatures* per quad. The corresponding eigenvectors yield curvature directions in each quad tangent plane.

The expected relationships hold between the principal curvatures, fundamental forms, and the mean and Gauss curvatures defined via the Steiner formula.

Lemma 3. *The following are true in the smooth and discrete case:*
1. $\mathcal{K} = k_1 k_2 = \det \mathrm{II} / \det \mathrm{I}$, *2.* $\mathcal{H} = \frac{1}{2}(k_1 + k_2)$,
3. $\mathrm{III} - 2\mathcal{H}\mathrm{II} + \mathcal{K}\mathrm{I} = 0$, *and* *4.* $A(f,f)^2 = \det \mathrm{I}$.

Constant curvature quad meshes

It turns out that many integrable geometries are edge-constraint quad meshes of the appropriate curvature; an example of non integrable geometry is recovered, too. For more details see [6].

Theorem 1. *The following previously defined algebraic quad meshes are edge-constraint of the appropriate* constant *curvature:*
1. *Discrete minimal* [2] *and their associated families,*
2. *Discrete cmc* [3] *and their associated families,*
3. *Discrete constant negative Gauß curvature* [1] *and their associated families,*

Theorem 2. *Discrete developable quad meshes built from planar strips* [7] *can be extended to edge-constraint quad meshes with vanishing Gauss curvature.*

References

[1] A. I. Bobenko and U. Pinkall. Discrete surfaces with constant negative Gaussian curvature and the Hirota equation. *Journal of Differential Geometry*, 43:527–611, 1996.

[2] A. I. Bobenko and U. Pinkall. Discrete isothermic surfaces. *Journal für die reine und angewandte Mathematik*, pages 187–208, 1996.

[3] A. I. Bobenko and U. Pinkall. Discretization of Surfaces and Integrable Systems. In A. I. Bobenko and R. Seiler, editors, *Discrete integrable geometry and physics*, pages 3–58. Oxford University Press, 1999.
[4] A. I. Bobenko, H. Pottmann, and J. Wallner. A curvature theory for discrete surfaces based on mesh parallelity. *Mathematische Annalen*, 348(1):1–24, 2010.
[5] A. I. Bobenko and Y. B. Suris. *Discrete Differential Geometry: Integrable Structure*, volume 98 of *Graduate Studies in Mathematics*. American Mathematical Society, 2008.
[6] T. Hoffmann, A. O. Sageman-Furnas, and M. Wardetzky. A discrete parametrized surface theory in $\mathbb{R}^3$. *arXiv preprint:1412.7293*.
[7] Y. Liu, H. Pottmann, J. Wallner, Y.-L. Yang, and W. Wang. Geometric modeling with conical meshes and developable surfaces. *ACM Transactions on Graphics*, 25(3):681–689, 2006.
[8] W. K. Schief. On a maximum principle for minimal surfaces and their integrable discrete counterparts. *Journal of Geometry and Physics*, 56(9):1484–1495, 2006.

Discrete line complexes and integrable evolution of minors

Wolfgang K. Schief
(joint work with Alexander I. Bobenko)

Two-parameter families of lines termed *line congruences* constitute fundamental objects in classical differential geometry [1]. Their importance in connection with the geometric theory of integrable systems has been well documented (see [2] and references therein). Recently, in the context of integrable discrete differential geometry [3], attention has been drawn to *discrete line congruences* [4], that is, two-parameter families of lines which are combinatorially attached to the vertices of a $\mathbb{Z}^2$ lattice. Discrete Weingarten congruences have been shown to lie at the heart of the Bäcklund transformation for discrete pseudospherical surfaces [5, 6, 7]. Discrete normal congruences have been used to define Gaussian and mean curvatures and the associated Steiner formula for discrete analogues of surfaces parametrised in terms of curvature coordinates [8, 9, 10]. Discrete line congruences have also found important applications in architectural geometry [11].

Here, we are concerned with the extension of discrete line congruences in a three-dimensional complex projective space $\mathbb{CP}^3$ to three-dimensional "lattices of lines", that is, maps of the form

$$\mathsf{l} : \mathbb{Z}^3 \to \{\text{lines in } \mathbb{CP}^3\}.$$

These three-parameter families of lines which may be termed *discrete line complexes* admit remarkable algebraic and geometric properties if one imposes canonical geometric constraints. Thus, a discrete line complex is *fundamental* if the two lines combinatorially attached to the vertices of any edge of the $\mathbb{Z}^3$ lattice intersect and the four points of intersection associated with any four edges of the same type of an elementary cube are coplanar. This is illustrated in Figure 1. It is observed that, equivalently, any four "diagonals" of the same type as depicted schematically in Figure 1 may be required to be concurrent. Fundamental line complexes are termed discrete rectilinear congruences in [4]. The following summary is based on [12] and a forthcoming publication.

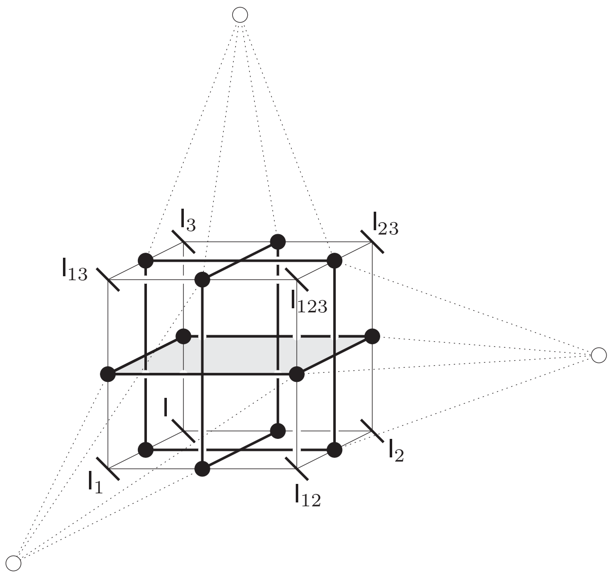

Figure 1

It turns out that if one parametrises generic lines of a fundamental line complex l in terms of homogeneous coordinates

$$\mathsf{V} = (1, M^{45,45}, M^{44}, M^{55}, M^{54}, M^{45})$$

of points in the classical (complexified) Plücker quadric Q^4 embedded in a five-dimensional complex projective space $\mathbb{CP}^5$ then the condition $\langle \mathsf{V}, \mathsf{V}\rangle = 0 \Leftrightarrow [\mathsf{V}] \in Q^4$ shows that $M^{45,45}$ is just the determinant of the matrix

$$\hat{\mathcal{M}} = \begin{pmatrix} M^{44} & M^{45} \\ M^{54} & M^{55} \end{pmatrix},$$

the entries of which obey the algebraic system (with $M^{ik}_l = M^{ik}|_{n_l \to n_l+1}$)

$$M^{ik}_l = M^{ik} - \frac{M^{il}M^{lk}}{M^{ll}}, \quad l \in \{1,2,3\}\backslash\{i,k\},$$

where the auxiliary quantities $M^{ik},\ i,k \notin \{4,5\}$ likewise satisfy the above system. This system of discrete evolution equations for the entries M^{ik} of the matrix $\mathcal{M} = (M^{ik})_{i,k=1,\dots,5}$ (and, in turn, its minors) is termed *M-system* in [12] and is integrable in the sense of multi-dimensional consistency [3]. In fact, it plays a privileged role in the algebraic and geometric theory of discrete and continuous integrable systems.

The algebraic characterisation of fundamental line complexes in terms of the M-system gives rise to the consideration of sub-geometries by virtue of admissible constraints on the matrix $\mathcal{M}$. If $\mathcal{M}$ is real then the Plücker quadric of signature $(3,3)$ is real and real fundamental line complexes are obtained. If $\mathcal{M}$ is Hermitian, that is, $\mathcal{M}^\dagger = \mathcal{M}$ then the associated subset of points in the complex Plücker quadric may be identified with the points of a real Lie quadric of signature $(4, 2)$. Hence, the admissible lines in $\mathbb{CP}^3$ are now interpreted as oriented spheres in a three-dimensional Euclidean space $\mathbb{R}^3$ and the intersection of lines becomes oriented contact of spheres, resulting in fundamental sphere complexes. Fundamental circle complexes on the plane are obtained by assuming that $\mathcal{M}$ is real and symmetric, that is, $\mathcal{M}^T = \mathcal{M}$, corresponding to the restriction of the Plücker quadric to a Lie quadric of signature $(3, 2)$. These sphere and circle complexes may also be defined geometrically due to a characterisation of fundamental line complexes in terms of correlations of $\mathbb{CP}^3$.

Fundamental circle complexes may be parametrised in terms of Bäcklund-related solutions of the master discrete CKP (dCKP) equation of integrable systems theory [13]. The latter was obtained by Kashaev [14] in the context of star-triangle moves in the Ising model. It constitutes a canonical reduction of the "hexahedron recurrence" proposed by Kenyon and Pemantle [15] which admits a natural interpretation in terms of cluster algebras and dimer configurations. It is noted that the dCKP equation interpreted as a local relation between the principal minors of a symmetric matrix $\mathcal{M}$ has been derived as a characteristic property by Holtz and Sturmfels [16] in connection with the 'principal minor assignment problem'.

In the spirit of Klein's Erlangen program, "deeper" reductions in Möbius, Laguerre and "hyperbolic" geometry may be obtained by imposing appropriate geometric constraints. These lead to the consideration of interesting classical and novel "circle theorems" such as (analogues of) Miquel's theorem and Clifford's chain of circle theorems. In the case of Möbius geometry, novel integrable hexagonal circle patterns have been brought to light.

References

[1] S.P. Finikov, *Theorie der Kongruenzen*, Akademie-Verlag, Berlin (1959).

[2] A. Doliwa, *Discrete asymptotic nets and W-congruences in Plücker line geometry*, J. Geom. Phys. **39** (2001) 9–29.

[3] A.I. Bobenko and Y.B. Suris, *Discrete differential geometry. Integrable structure*, Graduate Studies in Mathematics **98**, AMS, Providence (2008).

[4] A. Doliwa, P.M. Santini and M. Manas, *Transformations of quadrilateral lattices*, J. Math. Phys. **41** (2000), 944–990.

[5] R. Sauer, *Parallelogrammgitter als Modelle für pseudosphärische Flächen*, Math. Z. **52** (1950), 611-622.

[6] W. Wunderlich, *Zur Differenzengeometrie der Flächen konstanter negativer Krümmung*, Österreich. Akad. Wiss. math.-nat. Kl. S.-B. II **160** (1951), 39–77.

[7] A. Bobenko and U. Pinkall, *Discrete surfaces with constant negative Gaussian curvature and the Hirota equation*, J. Diff. Geom. **43** (1996), 527–611.

[8] W.K. Schief, *On the unification of classical and novel integrable surfaces. II. Difference geometry*, Proc. R. Soc. London A **459** (2003), 373–391.

[9] W.K. Schief, *On a maximum principle for minimal surfaces and their integrable discrete counterparts*, J. Geom. Phys. **56** (2006), 1484–1495.

[10] A.I. Bobenko, H. Pottmann and J. Wallner, *A curvature theory for discrete surfaces based on mesh parallelity*, Math. Annalen **348** (2010), 1–24.

[11] J. Wang, C. Jiang, P. Bompas, J. Wallner and H. Pottmann, *Discrete line congruences for shading and lighting*, SGP '13 Proceedings of the Eleventh Eurographics/ACMSIGGRAPH Symposium on Geometry Processing, The Eurographics Association and Blackwell Publishing Ltd. (2013), 53–62.
[12] A.I. Bobenko and W.K. Schief, *Discrete line complexes and integrable evolution of minors*, Proc. R. Soc. London A **471** (2015), 20140819 (23pp).
[13] W.K. Schief, *Lattice geometry of the discrete Darboux, KP, BKP and CKP equations. Menelaus' and Carnot's theorems*, J. Nonlinear Math. Phys. **10**, Supplement 2, (2003) 194–208.
[14] R.M. Kashaev, *On discrete three-dimensional equations associated with the local Yang-Baxter relation*, Lett. Math. Phys. **33** (1996), 389–397.
[15] R. Kenyon and R. Pemantle, *Double-dimers, the Ising model and the hexahedron recurrence*, arXiv:1308.2998 [math-ph] (2013).
[16] O. Holtz and B. Sturmfels, *Hyperdeterminantal relations among symmetric principal minors*, J. Algebra **316** (2007), 634–648.

Supercyclidic nets

Thilo Rörig
(joint work with Emanuel Huhnen-Venedey and Alexander I. Bobenko)

We present the extension of discrete conjugate nets, i.e., nets with planar quadrilateral faces, to piecewise smooth surface patchworks consisting of supercyclidic patches. Previously, such extensions have been studied for circular nets in [1] and discrete A-nets in [5]. For a detailed study and further references we refer to [2].

2D supercyclidic nets. Supercyclides are surfaces with a characteristic conjugate parametrization consisting of two families of conics such that the tangent planes along each conic envelop a quadratic cone.

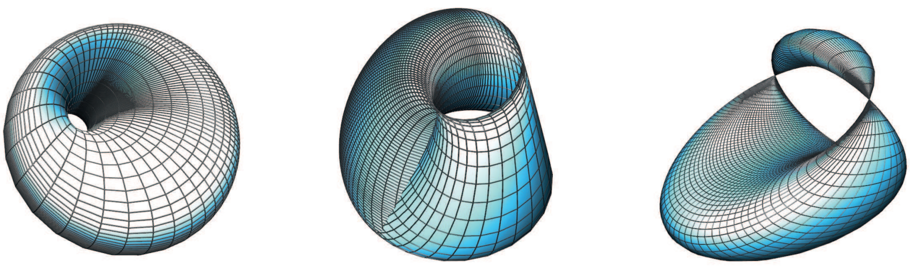

Figure 1. Three different types of supercyclides.

The image of the restriction of the characteristic conjugate parametrization to a rectangle yields a *supercyclidic patch*. These supercyclidic patches have the property that the corners lie in a plane and hence they can be attached to a Q-net, a discrete quadrilateral net with planar faces. We call a Q-net with adapted supercyclidic patches such that neighboring patches have the same tangent cones at the common conic segment a *supercyclidic net*. For an entire 2-dimensional Q-net with regular combinatorics we formulate the following Cauchy problem:

(1) Given the supporting Q-net $x : \mathbb{Z}^2 \to \mathbb{RP}^3$,
(2) two tangent congruences along two intersecting coordinate lines for each coordinate direction, and
(3) two conic splines, one along each coordinate lines.

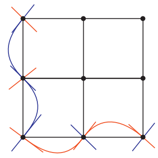

This problem has a unique solution and yields a piecewise smooth supercyclidic net adapted to the Q-net. The obtained tangent congruences are line systems adapted to Q-nets studied in [4] and fundamental line complexes in the sense of [3].

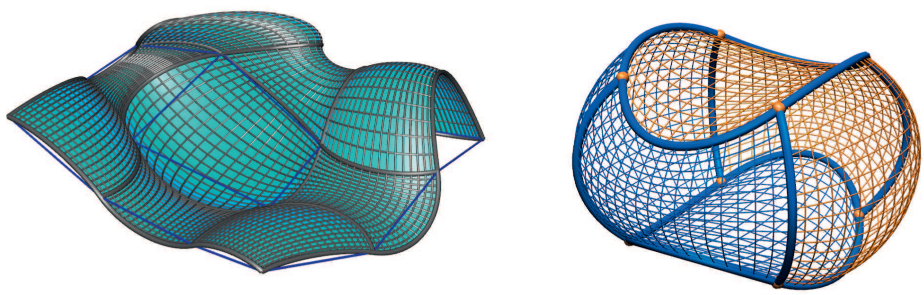

FIGURE 2. A 2-dimensional supercyclidic net and a 3-dimensional supercyclidic cube.

3D supercyclidic nets. In the 3-dimensional case we consider cubes with supercyclidic patches attached to the six faces. We show that three patches of a supercyclidic cube that share one vertex and cyclically sharing a common boundary curve each, determine the three opposite faces. Accordingly, the extension of a cube with planar faces to a supercyclidic cube is uniquely determined by the free choice of three patches. These supercyclidic cubes come with a refinement in all coordinate directions and yield piecewise smooth 3-dimensional coordinate systems.

Additionally, supercyclidic nets give rise to a 3D system. So from given initial data on three coordinate planes we can construct 3-dimensional supercyclidic nets. If we consider initial data on the coordinate axes as for 2D supercyclidic nets and generate the corresponding nets on the coordinate planes, then all surface patches will share the tangent cones along common edges in any 2D net parallel to the coordinate planes. Furthermore, the system is multidimensionally consistent.

Motivated by the theories of cyclidic and hyperbolic nets, we define fundamental transformations of supercyclidic nets by combination of the according smooth and discrete fundamental transformations of the involved SC-patches and supporting Q-nets, respectively.

It turns out that two mD supercyclidic nets are fundamental transforms if and only if they may be embedded as two consecutive layers of an $(m+1)$-dimensional supercyclidic net.

Frames of supercyclidic nets. One essential aspect of the theory is the extension of a given Q-net in $\mathbb{RP}^N$ to a system of circumscribed discrete torsal line systems. We present a description of the latter in terms of projective reflections that generalizes the systems of orthogonal reflections which govern the extension of circular nets to cyclidic nets by means of Dupin cyclide patches.

References

[1] A. I. Bobenko and E. Huhnen-Venedey. Curvature line parametrized surfaces and orthogonal coordinate systems: Discretization with Dupin cyclides. *Geometriae Dedicata*, 159(1):207–237, 2012.

[2] A. I. Bobenko and E. Huhnen-Venedey and T. Rörig. Supercyclidic nets Preprint, `http://arxiv.org/abs/1412.7422`, 2014.

[3] A. I. Bobenko and W. K. Schief. Discrete line complexes and integrable evolution of minors. Preprint, `http://arxiv.org/abs/1410.5794`, 2014.

[4] A. Doliwa, P. M. Santini, and M. Mañas. Transformations of quadrilateral lattices. *J. Math. Phys.*, 41(2):944–990, 2000.

[5] E. Huhnen-Venedey and T. Rörig. Discretization of asymptotic line parametrizations using hyperboloid surface patches. *Geometriae Dedicata*, 168(1):265–289, 2013.

Discrete Tangent Vector Fields as Linear Operators

Mirela Ben-Chen

(joint work with Omri Azencot, Steffen Weißmann, Frederic Chazal, Maks Ovsjanikov and Max Wardetzky)

Tangent vector fields on discrete surfaces are abundant in various applications in geometry processing. For example, tangent vector fields are used for guiding texture synthesis and quadrangular remeshing, as well as for representing the fluid's velocity in flow simulation on surfaces. Various choices are available for representing tangent vector fields on triangle meshes, such as an arrow per vertex or an arrow per face. In [1] we suggested instead to take the approach commonly used in differential geometry, and represent discrete tangent vector fields as *linear operators on discrete functions*. The main advantage of this approach is that discrete scalar functions can be represented using a finite basis, and then a discrete tangent vector field v can be represented by a square matrix D_v.

This methodology has a few immediate applications to geometry processing. First, consider for example the computation of the flow lines of a discrete vector field v, which is known to be a difficult problem. Using the operator D_v, we can define the pushforward of a function f_0 along the flow lines of v at time t as: $f(t) = \exp(tD_v)f_0$, where exp is the matrix exponential. Under a suitable choice of basis for discrete functions, the matrix D_v is sparse, and the previous computation can be done efficiently. Furthermore, the operator D_v fulfills a discrete version of integration by parts, and therefore this definition of pushforward guarantees that the integral of $f(t)$ over the mesh is independent of t if the vector field v is divergence free.

As an additional example, in [2] we showed how this approach can be used for simulating incompressible fluids on surfaces. For such fluids, the equations of motion can be formulated as $\partial_t \omega(t) = -D_{v(t)}\omega(t)$, where $v(t)$ is the divergence free velocity of the fluid at time t, and $\omega(t)$ is its vorticity. By taking a fixed velocity v^k per iteration k, we can similarly use the exponential of D_{v^k} to derive an efficient and simple simulation algorithm.

References

[1] O. Azencot, M. Ben-Chen, F. Chazal, and M. Ovsjanikov, *An operator approach to tangent vector field processing*, Computer Graphics Forum **32(5)** (2013), 73–82.

[2] O. Azencot, S. Weißmann, M. Ovsjanikov, M. Wardetzky and M. Ben-Chen, *Functional Fluids on Surfaces*, Computer Graphics Forum **33(5)** (2014), 237–246.

Cluster categories from dimer models

Alastair King

(joint work with B.T. Jensen, X. Su, K. Baur, R. Marsh)

The homogeneous coordinate ring $\mathcal{A}_k^n$ of the Grassmannian of k-planes in $\mathbb{C}^n$ is generated by Plücker coordinates (or minors) Δ_J, for $J \in \binom{n}{k}$, subject to quadratic Plücker relations. For example, in $\mathcal{A}_2^4$, there is the one short Plücker (or Ptolemy) relation

$$\Delta_{13}\Delta_{24} = \Delta_{12}\Delta_{34} + \Delta_{14}\Delta_{23}$$

As a motivating example of their theory of cluster algebras, Fomin-Zelevinsky [4] showed that $\mathcal{A}_2^n$ has a cluster structure of finite (Dynkin) type A_{n-3} in which the 'cluster variables' are the minors, arranged into 'clusters' each corresponding to a triangulation of an n-gon and for which the 'exchange relations' are the Ptolemy relations. Scott [6] generalised the cluster structure to all $\mathcal{A}_k^n$, showing that the only other finite type cases are for $k = 3$ and $n = 6, 7, 8$, where the Dynkin types are D_4, E_6, E_8.

One may observe that this numerology matches the fact that the plane curve singularity $x^k = y^{n-k}$ is simple in precisely these finite type cases and of the same type. One aim of this talk is to shed some light on this apparent coincidence.

Following the foundational work of Buan-Marsh *et al* [2], one looks for a category behind any cluster algebra, which naturally encodes the cluster structure. In particular, the cluster variables should be 'characters' of the rigid indecomposable objects in the category and the clusters correspond to maximal rigid objects. Technically speaking, this category should be a stably 2-Calabi-Yau Frobenius category, whose exact structure encodes the exchange relations in a particular way.

In the case of $\mathcal{A}_2^n$, it is possible to guess this category, inspired by the combinatorics of Coxeter-Conway frieze patterns [3], which can themselves now be understood in the broader context of cluster algebras. For example, for $\mathcal{A}_2^5$ a picture (technically, the Auslander-Reiten quiver) of the category is given in Figure 1. Note that the labels ij and ji represent the same object, with character Δ_{ij}, and the dashed squares commute.

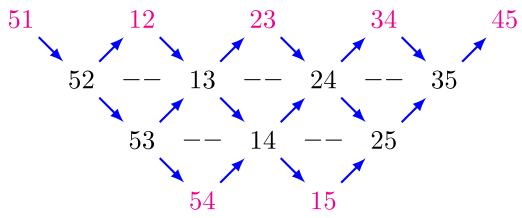

FIGURE 1. The cluster category for $\mathcal{A}_2^5$.

It is natural to ask how to realise this category as a module category and to guess, as verified in [5], that it is the category $\mathrm{CM}(B)$ of Cohen-Macaulay modules for the algebra $B = \mathrm{End}(P)$, where P is the direct sum of the projective-injective objects in the Frobenius category, e.g. the objects along the border of the 'frieze' in Figure 1. It can be easily checked that, in this $\mathcal{A}_2^n$ case, B is the path algebra of the quiver depicted on the right of Figure 2, modulo the relations $xy = yx$ and $x^2 = y^{n-2}$.

However, P must also be a summand of any maximal rigid object and so B will be an idempotent subalgebra eCe of any 'cluster tilted algebra' $C = \mathrm{End}(X_T)$, for the maximal rigid object X_T associated to a cluster/triangulation T. The question then arises as to how to determine the algebra C from the triangulation T . It is shown in [1] that this can be done by associating a dimer model to the triangulation, that is, a bipartite tiling of the dual n-gon, in the manner indicated by the example in Figure 2: the tiling vertices are the midpoints of the diagonals and there is one black triangular tile for each triangle in the triangulation. Next convert the dimer model to a quiver with relations by orienting the edges of the tiling so that they have black faces on the right and white faces on the left. The relations are commutation relations $p_a^+ - p_a^-$, for each internal arrow a, where the paths $p_a^\pm$ return from the head to the tail of arrow a around the left/right face of the tiling. The algebra C is the path algebra of the quiver modulo the ideal generated by these commutation relations. As expected, the algebra B is the idempotent subalgebra for the dimer model boundary, independent of triangulation.

For the case of $\mathcal{A}_k^n$ for $k \geqslant 3$, the above logic is run in reverse. We consider the algebra B defined by the same boundary quiver, but with relations $xy = yx$ and $x^k = y^{n-k}$. Then the category $\mathrm{CM}(B)$ has indecomposable rigid modules X_J, for each $J \in \binom{n}{k}$, which are the summands of a maximal rigid modules X_T, for each cluster of minors T. The combinatorial object that determines a cluster of minors T is a Postnikov alternating strand diagram, as illustrated in Figure 3. The relevant minors are associated to the alternating regions of the diagram by writing down the labels marking the beginning of the strands on the right of the

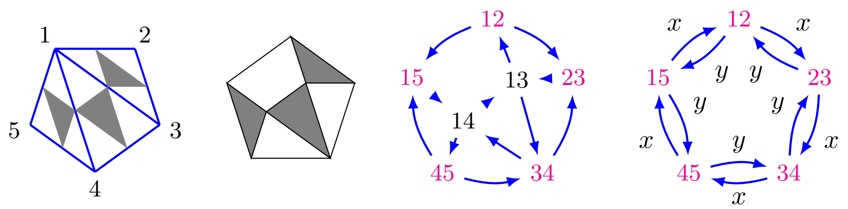

FIGURE 2. A triangulation, its associated dimer model and quiver, and the boundary quiver.

region. The quiver, and thus the associated dimer model, can be written down (as in Figure 4) by joining those minors whose alternating regions share a crossing point of two strands. In this case, one may prove that the algebra $C = \mathrm{End}(X_T)$ is, as before, the path algebra of the quiver modulo the ideal generated by the commutation relations coming from the tiles of the dimer model.

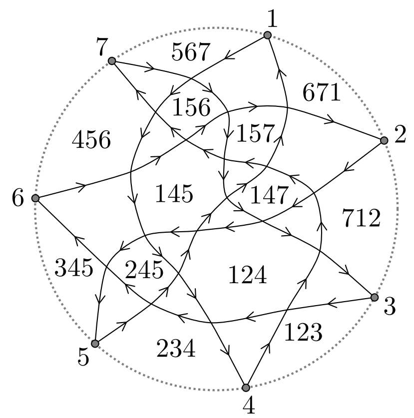

FIGURE 3. A Postnikov diagram, labelled by minors.

REFERENCES

[1] K. Baur, A. King, R. Marsh, *Dimer models and cluster categories of Grassmannians*, arXiv:1309.6524v2

[2] A.B. Buan, R. Marsh, M. Reineke, I. Reiten, G. Todorov *Tilting theory and cluster combinatorics* Adv. Math. **204** (2006) 572–618. (arXiv:math/0402054)

[3] J.H. Conway, H.S.M. Coxeter, *Triangulated polygons and frieze patterns* Math. Gaz. **57** (1973), 87–94 & 175–183.

[4] S. Fomin, A. Zelevinsky, *Cluster algebras II: Finite type classification*, Invent. Math. **154** (2003) 63–121. (arXiv:math/0208229)

[5] B.T. Jensen, A. King, X. Su, *A categorification of Grassmannian cluster algebras*, arXiv:1309.7301v2

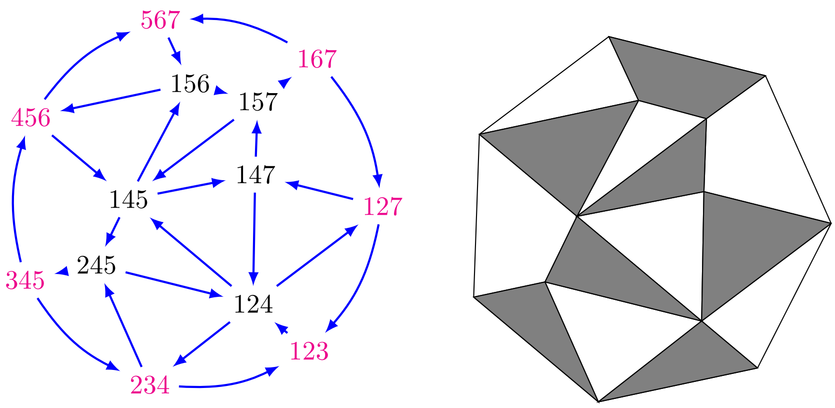

FIGURE 4. The associated quiver and dimer model.

[6] J. Scott, *Grassmannians and cluster algebras*, Proc. London Math. Soc. **92** (2006) 345–380. (arXiv:math/0311148)

Flag configurations and integrable systems.

VLADIMIR FOCK

The aim of this talk is to discuss certain the configuration spaces of flags. We are convinced that these space play a central role in discrete differential geometry in disguise of the space of lattices on a plane, configurations of points in a projective spaces and many others. We try to introduce some structure which we hope will be useful for discrete geometric applications.

Recall briefly a construction of [FG] of cluster parameterization of higher Teichmller spaces and $SL(N)$ local systems on 2D surfaces. The key ingredient is the consideration of the configuration space of complete flags in an N dimensional vector space H. Namely, associate a flag to every point of a rational projective line $\mathbb{Q}P^1$. The space of such flag configurations is obviously infinite dimensional. However one can impose a certain symmetry condition in order to make it finite dimensional. Namely, let $\mathcal{D} \in PSL(2,\mathbb{Z})$ be a finite index subgroup of the modular group such that the quotient of the upper half plane $\mathbb{H}^2$ by $\mathcal{D}$ is a surface $\mathcal{S}$. Consider now the configurations of flags invariant with respect to this subgroup. By invariance we mean that if we denote codimension i subspace of a flag corresponding to a point $\alpha \in \mathbb{Q}P^1$ by F^i_α then we require that for any $g \in \mathcal{D}$ there exists a linear map $\rho(g) : H \to H$ such that $F^i_{g(\alpha)} = \rho(g)F^i_\alpha$ for any i and α. Thus such flag configuration defines a homomorphism ρ from the fundamental group of $\mathcal{S}$ to the group $PGL(N)$ and thus a local system on Σ. As it is proven in [FG], the map from invariant flag configurations to local system is a finite covering in a general point. Therefore the description of local system is reduced to the description of flag configurations.

The aim of the present talk is to consider a relative of this construction. We claim that if we consider a finite flag configurations but in infinite dimensional space we get a phase spaces of a large class of integrable systems, defined by A.Goncharov and R.Kenyon in [GK] and (still conjecturally) the discrete integrable systems considered by V.Adler, A.Bobenko and Y.Suris in [ABS].

Let H be an infinite-dimensional vector space (with a topology of injective limit of finite dimensional spaces). A complete flag in H is a collection of subspaces $\ldots \subset F^1 \subset F^0 \subset F^{-1} \subset F^{-2} \subset \ldots$ enumerated by integers and such that F^i/F^{i+1} is one dimensional, $\lim_{n\to+\infty} F_i = 0$, and $\lim_{n\to+\infty} F_i = H$. Let now F^i_α be a collection of such flags enumerated by a finite set S and such that $\cap_\alpha F^0_\alpha = 0$ and the intersection is transversal. The space of such configurations is obviously infinite dimensional and in order to make it finite dimensional we need to impose an invariance condition. For this purpose fix a convex polygon Δ on the plane with integer vertices and sides in bijection with our set S. Denote by $a_\alpha \in \mathbb{Z}^2$ the sides of this polygon. Now consider flag configurations such that they are invariant with repect to an action of ρ of the Abelian group $\mathbb{Z}^2$ on H with $\rho(g)F^i_\alpha = F^{i+\langle g,a_\alpha\rangle}_\alpha$, where $\langle , \rangle$ is a nondegenerate pairing.

We claim that the space of such configurations is birationally equivalent to the space of pairs (planar algebraic curve given by a polynomial with Newton polygon Δ, line bundle of degree $g-1$ on it). Here g is the number of integer points inside Δ and at the same time the genus of the planar curve.

The construction of a curve and a line bundle on it starting from a flag configuration is essentially given by A.Goncharov and R.Kenyon in [GK]. The converse construction is described in [F] and goes as follows. Let Σ be compactification of an algebraic curve in $(\mathbb{C}^\times)^2$ given by the equation $P(\lambda,\mu) = \sum_{(ij)\in\Delta} c_{ij}\lambda^i\mu^j = 0$ and let $\mathcal{L} \in \mathrm{Pic}^{g-1}(\Sigma)$ be a line bundle of degree $g-1$ on it. Observe that for a generic polynomial $P(\lambda,\mu)$ the compactification points are in bijection with the sides (intervals between integer points on the boundary) of Δ and thus they are in bijection with the set S. Let H be the space of meromorphic section of $\mathcal{L}$ having poles only at the compactification points. Let F^i_α be the space of sections having zero of order at least i at the point α. The action of $\mathbb{Z}^2$ is given by multiplication of sections by monomials $\lambda^i\mu^j$.

The key observation to introduce coordinates on flag configurations is the following construction working both in finite and infinite dimensional cases. In both cases the set S has a canonical cyclic order. Consider a lattice $\mathbb{Z}^S$ generated by labels of the flags. The symmetry group $\mathcal{D}$ acts on this lattice preserving degree.

A *section* of the lattice is two-dimensional $\mathcal{D}$-invariant polygonal complex embedded into $\mathbb{R}^S$ and homeomorphic to the plane. The faces of this complex are polygons with vertices $[\boldsymbol{d}+\alpha_1, \boldsymbol{d}-\alpha_2, \ldots, \boldsymbol{d}+\alpha_{2l-1}, \boldsymbol{d}-\alpha_{2l}]$, where $\alpha_1,\ldots,\alpha_{2l}$ be any sequence of points of S such that $\alpha_i \neq \alpha_{i+1}$ and $\boldsymbol{d}$ be any lattice point of degree 0. We also require that the action of the group $\mathcal{D}$ on the section be conjugated to the action of $\mathcal{D}$ on the upper half plane in the first case and on a Euclidean plane in the second case. In particular it means that the quotient of the section by the group $\mathcal{D}$ is a finite complex homeomorphic to the surface $\mathcal{S}$ in the first case and to a two-dimensional torus in the second. The vertices of a section have either degree -1 (we will call them white) or degree 1 (we will call them black). One edge of every edge is white and another black.

For every white vertex $\boldsymbol{w} = \sum_\alpha w_\alpha \alpha$ associate a space $F^{\boldsymbol{w}} = \cap_\alpha F_\alpha^{w_\alpha}$. For every black vertex $\boldsymbol{b}$ associate a vector space $\ker \bigoplus_{\boldsymbol{w}-\boldsymbol{b}} F^{\boldsymbol{w}} \to H$, where the direct sum is taken over the neighbors of the vertex $\boldsymbol{b}$. For flags in general position both spaces are one dimensional and there is a natural map $F^{\boldsymbol{b}} \to F^{\boldsymbol{w}}$ for every edge connecting $\boldsymbol{b}$ and $\boldsymbol{w}$. Compositions of the maps around every face constitute a collection of numbers invariant under the action group $\mathcal{D}$. Therefore the collection of numbers on the faces of the quotient of the section by the group $\mathcal{D}$ constitute coordinates of the flag configuration.

The coordinate system is not unique since the choice of the section is not unique. Any two sections are related by a sequence of elementary transformations called *mutations*. Namely, every quadrilateral face $[\boldsymbol{d}+\alpha_1, \boldsymbol{d}-\alpha_2, \boldsymbol{d}+\alpha_3, \boldsymbol{d}-\alpha_4]$ can be replaced by a face $[\boldsymbol{d}'-\alpha_1, \boldsymbol{d}'+\alpha_2, \boldsymbol{d}'-\alpha_3, \boldsymbol{d}'-\alpha_4]$, where $\boldsymbol{d}' = \boldsymbol{d}+\alpha_1-\alpha_2+\alpha_3-\alpha_4$, and the adjacent faces, for example $[\ldots \boldsymbol{d}-\alpha_2, \boldsymbol{d}'+\alpha_1, \ldots]$ replaced by $[\ldots \boldsymbol{d}-\alpha_2, \boldsymbol{d}-\alpha_2+\alpha_1+\alpha_3, \boldsymbol{d}+\alpha_2+\alpha_1-\alpha_4, \boldsymbol{d}+\alpha_1, \ldots]$. Sequences of mutations leaving invariant the combinatorics of the section as a cell complex but changing its embedding in the lattice form a group coinciding with the mapping class group of the surface $\mathcal{S}$ in the first case and the group of discrete flows of the integrable system — a Abelian group of rank $\#S-3$ in the second.

References

[ABS] V.Adler, A. Bobenko, Yu. Suris, *Classification of integrable discrete equations of octahedron type.* Int. Math. Res. Not. IMRN 2012, no. 8, 1822–1889.

[GK] A.B.Goncharov and R.Kenyon, *Dimers and cluster integrable systems.* Ann. Sci. Éc. Norm. Supér. (4) 46(2013) , no. 5, 747-813. `arXiv:1107.5588`

[FG] V.V. Fock, A.B. Goncharov, *Moduli spaces of local systems and higher Teichmüller theory*, Publ. IHES vol. 103 nr.1, pp.1–221, 2006, `math.AG/0311149`

[FM] V.V.Fock and A.V.Marshakov *Loop groups, Clusters, Dimers and Integrable systems.* `arXiv:1401.1606.`

[F] V.V.Fock *Inverse spectral problem for GK integrable system.* `arXiv:1503.0289`.

Circle patterns and confocal conics

Arseniy Akopyan

(joint work with Alexander Bobenko)

1. IC-net

We consider maps of the square grid to the plane $f : \mathbb{Z}^2 \to \mathbb{R}^2$ and use the following notations:

- $f_{i,j} = f(i,j)$ for the vertices of the net,
- $\square_{i,j}^c$ for the quadrilateral $(f_{i,j}, f_{i+c,j}, f_{i+c,j+c}, f_{i,j+c})$ which we call a *net-square*,
- $\square_{i,j}$ for the net-square $\square_{i,j}^1$ which we call a *unit net-square*.

Definition 1. An IC-net (inscribed circular net) is a map $f : \mathbb{P} \to \mathbb{R}^2$ satisfying the following conditions:

(i) For any integer i the points $\{f(i,j)|j \in \mathbb{Z}\}$ lie on a straight line preserving the order, i.e the point $f(i,j)$ lies between $f(i,j-1)$ and $f(i,j+1)$. The same holds for points $\{f(i,j)|i \in \mathbb{Z}\}$. We call these lines the *lines of the IC-net.*

(ii) all unit net-squares $\square_{i,j}$ are circumscribed. We denote the inscribed circle of $\square_{i,j}$ by $\omega_{i,j}$ and its center by $o_{i,j}$.

Theorem 1. *Let f be an IC-net. Then the following properties hold:*

(i) All lines of the IC-net f touch some conic α (possibly degenerate).

(ii) The points $f_{i,j}$, where $i + j = \text{const}$ lie on a conic confocal with α. As well the points $f_{i,j}$, where $i - j = \text{const}$ lie on a conic confocal with α.

(iii) All net-squares of f are circumscribed.

(iv) In any net-square with even sides the midlines have equal lengths:

$$|f_{i-c,j}f_{i+c,j}| = |f_{i,j-c}f_{i,j+c}|.$$

(v) The cross ratio

$$cr(f_{i,j_1}, f_{i,j_2}, f_{i,j_3}, f_{i,j_4}) = \frac{(f_{i,j_1} - f_{i,j_2})(f_{i,j_3} - f_{i,j_4})}{(f_{i,j_2} - f_{i,j_3})(f_{i,j_4} - f_{i,j_1})}$$

is independent of i. The cross ratio $cr(f_{i_1,j}, f_{i_2,j}, f_{i_3,j}, f_{i_4,j})$ is independent of j.

(vi) Consider the conics C_k that contain the points $f_{i,j}$ with $i + j = k$ (see (ii)). Then for any $l \in \mathbb{Z}$ there exists an affine transformation $A_{k,l} : C_k \to C_{k+2l}$ such that $A_{k,l}(f_{i,j}) = f_{i+l,j+l}$. The same holds for the conics through the points $f_{i,j}$ with $i - j = \text{const}$.

(vii) The net-squares $\square^c_{i,j}$ and $\square^{c+2l}_{i-l,j-l}$ are perspective.

(viii) Let $\omega_{i,j}$ be the inscribed circle of the unit net-square $\square_{i,j}$. Consider the cone in $\mathbb{R}^3$ intersecting the plane along $\omega_{i,j}$ at constant oriented angle (all the apexes $a_{i,j}$ of these cones lie in one half-space). Then all the apexes $a_{i,j}$ lie on one-sheeted hyperboloid.

(ix) Let $o_{i,j}$ be the center of the circle $\omega_{i,j}$. Then all $o_{i,j}$ with $i + j = \text{const}$ lie on a conic, and $o_{i,j}$ with $i - j = \text{const}$ also lie on a conic.

(x) The centers $o_{i,j}$ of circles of an IC-net build a projective image of an IC-net.

Theorem 2 (Construction of IC-net)**.** *IC-nets considered up to Euclidean motions and homothety build a real four-dimensional family. An IC-net is uniquely determined by two neighboring circles $\omega_{0,0}$, $\omega_{1,0}$ and their tangent lines ℓ_0, ℓ_1, ℓ_2, m_0, m_1.*

2. Checkerboard IC-net

Definition 2. A checkerboard IC-net is a map $f : \mathbb{P} \to \mathbb{R}^2$ satisfying the following conditions:

(1) For any integer i the points $\{f_{i,j}|j \in \mathbb{Z}\}$ lie on a straight line preserving the order, i.e the point $f_{i,j}$ lies between $f_{i,j-1}$ and $f_{i,j+1}$. The same holds

for points $\{f_{i,j} | i \in \mathbb{Z}\}$. We call these lines the *lines of the checkerboard IC-net.*

(2) For any integer i and j, such that $i + j$ is even the quadrilateral with verities $f_{i,j}$, $f_{i+1,j}$, $f_{i+1,j+1}$, $f_{i,j+1}$ is circumscribed.

We call quadrilaterals $\square_{i,j}$ with vertices $f_{i,j}$, $f_{i+1,j}$, $f_{i+1,j+1}$, $f_{i,j+1}$ with even $i+j$ *unit net-squares* of checkerboard IC-net. The quadrilaterals $\square^c_{i,j}$ with vertices $f_{i,j}$, $f_{i+c,j}$, $f_{i+c,j+c}$, $f_{i,j+c}$ with even $i+j$ and odd c we call *net-squares.*

Theorem 3. *Let f be a checkerboard IC-net. Then the following properties hold:*

(i) All net-squares are circumscribed.

(ii) Net-squares $\square^c_{i,j}$ and $\square^{c+2l}_{i-l,j-l}$, where l is odd, are perspective.

(iii) The points $f_{i,j}$, where $i + j = \text{const}$ lie on a conic. The points $f_{i,j}$, where $i - j = \text{const}$ lie on a conic as well.

(iv) (Ivory-type theorem) We define the distance $d_C(\square_{a,b}, \square_{c,d})$ between two unit net-squares $\square_{a,b}$ and $\square_{c,d}$ of a checkerboard net as the distance between the tangent points on a common exterior tangent line to the circles $\omega_{a,b}$ and $\omega_{c,d}$ inscribed in $\square_{a,b}$ and $\square_{c,d}$ respectively. In case $a = c$ or $b = d$ these tangent lines are the lines of the checkerboard IC-net.

For any $(i, j) \in \mathbb{Z}^2$, with even $i + j$ and any integer even c one has

$$d_C(\square_{i-c,j}, \square_{i+c,j}) = d_C(\square_{i,j-c}, \square_{i,j+c}).$$

(v) Let $\omega_{i,j}$ be the inscribed circle of the unit net-square $\square_{i,j}$. Consider the cone in $\mathbb{R}^3$ intersecting the plane along $\omega_{i,j}$ at constant oriented angle (all the apexes $a_{i,j}$ of these cones lie in one half-space). Then all the apexes $\{a_{i,j} | i + j = 4n, n \in \mathbb{Z}\}$ lie on one-sheeted hyperboloid. The the apexes $\{a_{i,j} | i + j = 4n + 2, n \in \mathbb{Z}\}$ lie on one-sheeted hyperboloid as well.

(vi) The centers $o_{i,j}$ of the incircles of a checkerboard IC-net build a circle-conical net, i.e. a net that is simultaneously circular and conical. Recall that circular nets are the nets with circular quadrilaterals $(o_{i,j}o_{i+1,j+1}o_{i,j+2}o_{i-1,j+1})$ and conical nets in plane are characterized by the condition that the sums of two opposite angles at a vertex are equal (and equal to π).

The construction of IC-nets is based on the following theorem.

Theorem 4 (checkerboard incircles incidence theorem)**.** *Consider a quadrilateral which is cut by two sets of four lines in 25 quadrilaterals. Color the quadrilaterals in a checkerboard pattern with black quadrilaterals at the corners. Assume that all black quadrilaterals except one at a corner are circumscribed. The the the last black quadrilateral at the corner (thirteenth quadrilateral) is also circumscribed.*

3. Checkerboard inspherical nets in $\mathbb{R}^3$

There is a natural generalization of checkerboard IC-net in three (and higher) dimension. Let $\mathbb{P}^3$ be a parallelepiped in $\mathbb{Z}^3$.

Definition 3. A checkerboard IS-net is a map $f : \mathbb{P} \to \mathbb{R}^3$ satisfying the following conditions:

(i) All points of lines parallel to coordinate axis f maps to a point on a line with the same order.

(ii) For any integer i the points $\{f_{i,j,k}|k \in \mathbb{Z}\}$ lie on a straight line preserving the order, i.e the point $f_{i,j,k}$ lies between $f_{i,j,k-1}$ and $f_{i,j,k+1}$. The same holds for points $\{f_{i,j,k}|i \in \mathbb{Z}\}$ and $\{f_{i,j,k}|j \in \mathbb{Z}\}$. We call these lines the *lines of the checkerboard IS-net.*

(iii) Image of any unit cube of $\mathbb{P}^3$ which all coordinate even or odd is circumscribed polytope.

By $\square^c_{i,j,k}$ we denote a net-cube with smallest vertex $f_{i,j,k}$ (having minimal coordinate in each axis) and edge length c. Images of lines in $\mathbb{Z}^3$ parallel to coordinate axis we denote by $\ell^x_{i,j}$, where x denote the axis (it could be y or z) and i, j is coordinate of line in perpendicular plane.

Theorem 5. *(i) All net-cubes of IS-net are circumscribed.*

(ii) The net cubes $\square^c_{i,j,k}$ and $\square^{c+4s+2}_{i-2s-1,j-2s-1,k-2s-1}$ are perspective.

(iii) All net-cubes are projective cubes, i.e. projective images of the standard cube.

(iv) The lines $\ell^z_{i,j}$, where $i + j = const$ lie on hyperboloid of one sheet. The same holds for lines with $i - j = const$ and for lines with other directions.

Theorem 6 (9 inspheres incidence theorem)**.** *Suppose combinatorial cube $\square$ in $\mathbb{R}^3$ cut by 6 planes on 27 combinatorial cubes. Suppose the central and seven of the corner cells are circumscribed. Then the last corner cell is also circumscribed.*

We mention here a claim of independent interest which we used in the proof of the Theorem 5.

Theorem 7. *Suppose combinatorial cube $\square$ in $\mathbb{R}^d$ is cut by $2d$ hyperplanes on 3^d combinatorial cubes. Suppose the central and 2^d corner cells are circumscribed. Then the cube $\square$ is also circumscribed.*

Remark. Everything from the previous theorems, works well in case of Hyperbolic plane or on Sphere.

A discrete uniformization theorem for polyhedral surfaces

Feng Luo

(joint work with David Gu, Jian Sun, Tianqi Wu)

The Poincare-Koebe uniformization theorem for Riemann surfaces is one of the pillars in the last century mathematics. It states that given any Riemannian metric on any connected surface, there exists a complete constant curvature Riemannian metric conformal to the given one. The uniformization theorem has a wide range of applications within and outside mathematics. For instance, the uniformization theorem provides a canonical way to parameterize a simply connected Riemann surface. This special feature has been used in computer graphics and imaging processing. Polyhedral surfaces are ubiquitous due to digitization. Classifying and categorizing them appear to be an urgent task. On the other hand, algorithmically implementation of the classical uniformization theorem for polyhedral surfaces appears to be difficult. For instance there is no known algorithm to decide if the boundaries of two tetrahedra, considered as Riemann surfaces, are related by a conformal map preserving vertices. There has been much work on establishing various discrete versions of the uniformization theorem for discrete or polyhedral surfaces. A key step in discretization is to define the concept of discrete conformality. The most prominent discrete uniformization theorem is probably Andreev-Koebe-Thurston's circle packing theorem [10], [9]. Unfortunately not all polyhedral surfaces can be canonically packed by circles. The purpose of this report is to introduce a discrete conformality for polyhedral metric surfaces and to establish a discrete uniformization theorem within the category of polyhedral metrics. Two main features of the discrete conformality are the following. First, the discrete conformality is algorithmic and second, there exists a finite dimensional (convex) variational principle to find the discrete uniformization metric.

A closed surface S together with a non-empty finite subset of points $V \subset S$ will be called a *marked surface*. A triangulation $\mathcal{T}$ of a marked surface (S, V) is a topological triangulation of S so that the vertex set of $\mathcal{T}$ is V. We use $E = E(\mathcal{T})$, $V = V(\mathcal{T})$ to denote the sets of all edges and vertices in $\mathcal{T}$ respectively. A (Euclidean) *polyhedral metric* on (S, V), to be called *PL metric* on (S, V) for simplicity, is a flat cone metric on (S, V) with cone points in V. For instance boundaries of convex polytopes are PL metrics on $(\mathbf{S}^2, V)$. The *discrete curvature* of a PL metric d is the function $K_d : V \to (-\infty, 2\pi)$ sending a vertex v to 2π less the cone angle at v. For a closed surface S, it is well known that the Gauss-Bonnet theorem $\sum_{v \in V} K_d(v) = 2\pi\chi(S)$ holds. If $\mathcal{T}$ is a triangulation of (S, V) with a PL metric d for which all edges in $\mathcal{T}$ are geodesic, we say $\mathcal{T}$ is *geometric* in d and d is a PL metric on $(S, V, \mathcal{T})$. In this case, we can represent the PL metric d by the length function $l_d : E(\mathcal{T}) \to \mathbb{R}_{>0}$ sending an edge to its length.

Each polyhedral metric d on (S, V) has a natural *Delaunay triangulation* $\mathcal{T}_d$ which is a geometric triangulation with vertices V so that for each edge, the sum of two opposite angles facing e is at most π.

Definition 1. Two PL metrics d and d' on a marked closed surface (S, V) are *discrete conformal* if there is a sequence of PL metrics $d_1 = d, d_2, ..., d_n = d'$ and a sequence of triangulations $\mathcal{T}_1$, $\mathcal{T}_2$, ..., $\mathcal{T}_n$ of (S, V) so that

(a) each $\mathcal{T}_i$ is Delaunay in d_i,

(b) if $\mathcal{T}_i \neq \mathcal{T}_{i+1}$, then there is an isometry h_i from (S, V, d_i) to (S, V, d_{i+1}) so that h_i is homotopic to the identity map on (S, V), and

(c) if $\mathcal{T}_i = \mathcal{T}_{i+1}$, there is a function $u_i : V \to \mathbb{R}_{>0}$ so that for each edge $e = vv'$ in $\mathcal{T}_i$, the lengths $l_{d_i}(vv')$ and $l_{d_{i+1}}(vv')$ of e in d_i and d_{i+1} are related by

$$l_{d_{i+1}}(vv') = l_{d_i}(vv')u_i(v)u_i(v'). \tag{1}$$

The main theorems we proved are:

Theorem 1.([3]) *Given any PL metric d on a closed marked surface (S, V) and any $K^* : V \to (-\infty, 2\pi)$ so that $\sum_{v \in V} K^*(v) = 2\pi\chi(S)$, there exists a PL metric d^*, unique up to scaling, so that*

(a) d^* is discrete conformal to d, and

(b) the discrete curvature $K_{d^*} = K^*$.

Furthermore, the PL metric d^* can be found by a finite dimensional variational principle.

Theorem 2.([4]) *Given two PL metrics on a closed marked surface (S, V) whose edge lengths are algebraic numbers, there exists an algorithm to decide if they are discrete conformal.*

Theorem 2 is proved in our joint work with Ren Guo in [4]. Similar theorems for hyperbolic polyhedral surfaces have been established in [4].

Recall that two PL metrics d, d' on (S, V) are *Teichüller equivalent* if there exists an isometry $h : (S, V, d) \to (S, V, d')$ so that h is homotopic to the identity on (S, V). There are two major steps involved in the proof of theorem 1. In the first step, we show that for any PL metric d, the space $Dc(d)$ of all Teichmüller equivalance classes of PL metrics d' which are discrete conformal to d is C^1 diffeomorphic to the Euclidean space $\mathbb{R}^V$. This step uses the work of Penner [6], Rivin [7] and Bobenko-Pinkall-Springborn [2].

In the second step, we show that the discrete curvature map $K : Dc(d)/\mathbb{R}_{>0} \to (-\infty, 2\pi)^V \cap \{x \in \mathbb{R}^V | \sum_v x(v) = 2\pi\chi(S)\}$ is a homeomorphism. The local injectivity of K is proved using a variational principle developed in [5]. A theorem of Akiyoshi [1] together with a degeneration analysis shows that the map K is closed. Therefore, by the standard continuity method, we conclude that K is a bijection which is equivalent to theorem 1.

An interesting remaining issue is whether discrete conformality approximates the smooth conformality. The situation is very similar to Thurston's circle packing approximation to smooth conformality. Thurston's discrete Riemann mapping conjecture was established by Rodin-Sullivan's work [8].

A discrete Riemann mapping conjecture. *Suppose Ω is a Jordan domain in the complex plane. Take three distinct points p, q, r in the boundary of Ω. For each $\epsilon > 0$, let Ω_ϵ be a maximum simply connected domain in Ω which has a triangulation A_ϵ by equilateral triangles of edge length ϵ. Take three vertices $p_\epsilon, q_\epsilon, r_\epsilon$ in the boundary of Ω_ϵ so that Euclidean distances $d(p, p_\epsilon)$, $d(q, q_\epsilon)$ and $d(r, r_\epsilon)$ are less than 2ϵ. Let the metric double of $(\Omega_\epsilon, A_\epsilon)$ along the boundary be the polyhedral 2-sphere $(\mathbf{S}^2, B_\epsilon, d_\epsilon)$. Using theorem 1, one produces a new polyhedral metric $(\mathbf{S}^2, T_\epsilon, d^*_\epsilon)$ so that (1) its area is $\sqrt{3}/2$, (2) d^*_ϵ is discrete conformal to d_ϵ, (3) the discrete curvatures of d^*_ϵ at $p_\epsilon, q_\epsilon, r_\epsilon$ are $4\pi/3$ and (4) the discrete curvatures of d^*_ϵ at all other vertices are zero. Then as ϵ tends to 0, $(\mathbf{S}^2, T_\epsilon, d^*_\epsilon)$ converges to the metric double of the unit equilateral triangle.*

Numerical evidences supporting this conjecture are very strong.

References

[1] Hirotaka Akiyoshi, *Finiteness of polyhedral decompositions of cusped hyperbolic manifolds obtained by the Epstein-Penner's method*. Proc. Amer. Math. Soc. 129 (2001), no. 8, 2431–2439.
[2] Alexander Bobenko, Ulrich Pinkall, Boris Springborn, *Discrete conformal maps and ideal hyperbolic polyhedra*. arXiv:1005.2698
[3] David Gu, Feng Luo, Jian Sun, Tianqi Wu, *A discrete uniformization theorem for polyhedral surfaces*. arXiv:1309.4175
[4] David Gu, Ren Guo, Feng Luo, Jian Sun, Tianqi Wu, *A discrete uniformization theorem for polyhedral surfaces II.* arXiv.org:1401.4594
[5] Feng Luo, *Combinatorial Yamabe flow on surfaces*. Commun. Contemp. Math. 6 (2004), no. 5, 765–780.
[6] Robert C. Penner, *The decorated Teichmller space of punctured surfaces*. Comm. Math. Phys. 113 (1987), no. 2, 299–339.
[7] Rivin, Igor, *Euclidean structures on simplicial surfaces and hyperbolic volume.* Ann. of Math. (2) 139 (1994), no. 3, 553–580.
[8] Rodin, Burt, Sullivan, Dennis, *The convergence of circle packings to the Riemann mapping.* J. Differential Geom. 26 (1987), no. 2, 349–360.
[9] Stephenson, Kenneth, *Introduction to circle packing. The theory of discrete analytic functions.* Cambridge University Press, Cambridge, 2005. xii+356 pp.
[10] W. Thurston, *Geometry and topology of 3-manifolds*, Princeton University, 1980.

Spectral Discrete Exterior Calculus

Yiying Tong

(joint work with Beibei Liu, Yuanzhen Wang, Gemma Mason, Julian Hodgson, Mathieu Desbrun and Kun Zhou)

As a generalization of spectral analysis from regular grids in Euclidean spaces to curved spaces, manifold harmonics (MH) [1] has been used in a wide range of applications, including geometry processing and surface correspondences. Linking analysis of scalar fields to vector fields and differential forms, discrete exterior calculus (DEC) [2] has proven to be a flexible computational device for efficient calculation performed on simplicial meshes. We propose to combine the power of the two tools into an efficient and effective toolkit for spectral analysis on meshes.

On surfaces, we first build the basis functions of differential forms, through manifold harmonics of scalar fields and harmonic 1-forms. Then, the basic operators in exterior calculus reduce to simple matrices. Specifically, we start with the scalar Laplacian Δ^0 in DEC (the cotan formula) on a triangle surface mesh containing a single genus-g connected component, and calculate the smallest $m+1$ eigenvalues of $d{*}d\Phi_i = -\kappa_i^2 {*}\Phi_i$, where κ_i corresponds to the i-th smallest spatial frequency (wave number), and Φ_i is the associated eigenfunction. For instance, with the total surface area rescaled to 1, the 0-th frequency ($\kappa_0 = 0$) eigenfunction is always $\Phi_0 = [1\ 1 \ldots 1]^T$. The bases for the low frequency differential forms can be assembled as

$$\begin{array}{ll} \text{0-form basis:} & [\Phi_0\ \Phi_1\ \ldots\ \Phi_m], \\ \text{1-form basis:} & [h_1 \ldots h_{2g}\ \frac{d\Phi_1}{\kappa_1} \ldots \frac{d\Phi_m}{\kappa_m}\ \frac{*d\Phi_1}{\kappa_1} \ldots \frac{*d\Phi_m}{\kappa_m}], \\ \text{2-form basis:} & [*\Phi_0\ *\Phi_1\ \ldots\ *\Phi_m], \end{array}$$

where h_i's provide a basis for the harmonic 1-forms. The Hodge star $*h_i$ is a linear combination of h_i's, which can be calculated through the period matrix [3] when h_i's are computed based on the cohomology basis. For simplicity, we assume trivial topology in the following discussion. The Hodge star operators $*$ for 0-forms and 2-forms become the identity matrix $*^0 = *^2 = I_{m+1}$, and $*^1$ can be expressed as

$$*^1 = \begin{pmatrix} 0 & -I_m \\ I_m & 0 \end{pmatrix}.$$

By using the diagonal matrix assembled from the wave numbers, $D = \text{diag}[\kappa_1 \ldots \kappa_m]$, we can express the exterior derivatives as

$$d^0 = \begin{pmatrix} (0\ldots0)^T & D \\ (0\ldots0)^T & \mathbf{0} \end{pmatrix},\ d^1 = \begin{pmatrix} 0 & 0\ldots0 \\ \mathbf{0} & D \end{pmatrix},$$

where $\mathbf{0}$ denotes a matrix of the same size as D with every entry equal to 0. These operators reflect the fact that differential in spectral domain is achieved by multiplication of frequencies.

In volumetric meshes, we cannot construct the bases solely from the 0-form bases. Instead, we extend the bases proposed in [4] by solving for eigenvalues of the 1-form Laplacian, $\Delta^1\Psi_i = -\mu_i^2\Psi_i$. Note that the gradients of 0-form basis functions $d\Phi_i/\kappa_i$ are eigen 1-forms since $d\Delta = \Delta d$. Thus the lowest m_0 frequencies for 0-forms κ_i's form a subset of the m_1 frequencies for 1-forms μ_i's, with m_1 chosen as the smallest integer satisfying $\mu_{m_1} \geqslant \kappa_{m_0}$. For a typical tetrahedral mesh, $m_1 \approx 3m_0$. Assuming trivial topology, we can reorganize the 1-form basis by categorizing the basis 1-forms into those of the form $d\Phi_i/\kappa_i$ (the m_0 gradient fields) and the rest (the $m_1 - m_0$ curl fields). Thus, the bases of all differential forms can be expressed as

0-form basis: $[\Phi_0\ \Phi_1\ \ldots\ \Phi_{m_0}]$,

1-form basis: $[\frac{d\Phi_1}{\kappa_1} \ldots \frac{d\Phi_{m_0}}{\kappa_{m_0}}\ \Psi_1 \ldots \Psi_{m_1-m_0}]$,

2-form basis: $[*\frac{d\Phi_1}{\kappa_1} \cdots * \frac{d\Phi_{m_0}}{\kappa_{m_0}}\ *\Psi_1 \cdots *\Psi_{m_1-m_0}]$,

3-form basis: $[*\Phi_0\ *\Phi_1\ \ldots\ *\Phi_{m_0}]$.

With these bases, all Hodge star $*$ operators become the identity matrices. Assembling the eigenvalues as $D_0 = \text{diag}[\kappa_1 \ldots \kappa_{m_0}]$ and $D_1 = \text{diag}[\mu_1 \ldots \mu_{m_1-m_0}]$, we can express the exterior derivatives as

$$d^0 = \begin{pmatrix} (0\ldots0)^T & D_0 \\ (0\ldots0)^T & \mathbf{0} \end{pmatrix},\ d^1 = \begin{pmatrix} \mathbf{0} & \mathbf{0} \\ \mathbf{0} & D_1 \end{pmatrix},\ d^2 = \begin{pmatrix} 0\ldots0 & 0\ldots0 \\ D_0 & \mathbf{0} \end{pmatrix}.$$

With the Hodge star and exterior derivative expressed in these simple forms, differential and integral can be performed efficiently for the spaces of low frequency differential forms. In addition, Helmholtz-Hodge decomposition becomes simple projections to different subsets of the coefficients in the bases. Notice that, in 3D or 2D case with boundaries, the boundary conditions for k-forms and $n-k$-forms must match to get simple operators.

References

[1] Bruno Vallet and Bruno Lévy. Spectral geometry processing with manifold harmonics. In *Computer Graphics Forum*, volume 27, pages 251–260. Wiley Online Library, 2008.

[2] M. Desbrun, E. Kanso, and Y. Tong. Discrete differential forms for computational modeling. *Discrete differential geometry*, pages 287–324, 2008.

[3] Xianfeng Gu and Shing-Tung Yau. Computing conformal structure of surfaces. *arXiv preprint cs/0212043*, 2002.

[4] Tyler De Witt, Christian Lessig, and Eugene Fiume. Fluid simulation using Laplacian eigenfunctions. *ACM Trans. Graph.*, 31(1):10:1–10:11, February 2012.

Modelling of developables and curved folds

Johannes Wallner

(joint work with Helmut Pottmann, Chengcheng Tang, Pengbo Bo)

We have been studying the problem of interactive geometric modelling of piecewise C^2 surfaces which either consist of intrinsically flat (developable) pieces or are entirely flat. This class of surfaces corresponds to shapes which can be made from paper or from sheet metal, either with or without cutting along the creases. In order to make this problem computationally tractable we use two facts:

— (i) developables decompose into ruled pieces definable by a correspondence between space curves. This is a simplified statement of Hartmann and Nirenberg's theorem on existence of generators on intrinsically flat C^2 surfaces;

— (ii) curves in space may be approximated, together with their derivatives, by polynomial splines of degree $\geqslant 2$.

These facts are the foundation of the following simplification of the modeling problem. We study composite surfaces which are built from polygonal planar faces and from *spline developables*. The latter is a parametric surface of the kind $x : [0,1]^2 \to \mathbb{R}^3$, $x(u,v) = (1-v)a(u) + vb(u)$ which has zero Gaussian curvature, and where both a, b are polynomial spline curves contained in the same spline space. The individual pieces of such a composite surface join each other either along a spline curve or along a straight line segment.

The shape of such a surface is stored in the combinatorics of its decomposition together with *control points*, i.e., coefficients of the boundary curves in the spline basis. The control points are not arbitrary but must be chosen such that the composite surface obeys the following conditions:

(1) developability of its smooth parts;
(2) if required, developability (intrinsic flatness) along creases;
(3) if required, developability in vertices, i.e., absence of cone points;
(4) further side conditions imposed by the problem at hand.

Since spline spaces are finite-dimensional, condition (1) amounts to a finite number of equations imposed on the control points of an individual spline developable. The number of equations is determined by the polynomial degree of the condition $\det(\dot{a}, \dot{b}, a - b) = 0$ expressing vanishing Gaussian curvature. Similar considerations apply to conditions (2)–(4). We have thus turned the problem of modeling with developables into a finite number of equations. As it turns out, this system can be solved at interactive speeds despite being nonlinear, under-determined, and very likely inconsistent at the same time. This is due to the fact that by introducing auxiliary variables like spline normal vector fields, we can make all equations quadratic while still retaining sparsity. Tang et al. [3] have shown how to solve such a system of equations via "energy-guided projection", which is essentially a regularized Newton method.

Taking the above as a guide, we were able to implement a modeling system for developables. Items such as the planar unfolding of surfaces are added via appropriate numerical approximations (meshes). In particular we demonstrate the capabilities of the implementation by recreating some of the popular curved-folding objects of art created by David Huffman and by Erik Demaine, see e.g. [1].

References

[1] E. Demaine, M. Demaine, D. Koschitz. *Reconstructing David Huffman's legacy in curved-crease folding.* In Origami^5. A.K. Peters 2011, pp. 39–52.

[2] C. Tang, P. Bo, J. Wallner, H. Pottmann, *Interactive design of developable surfaces*, preprint.

[3] C. Tang, X. Sun, A. Gomes, J. Wallner, and H. Pottmann, *Form-finding with polyhedral meshes made simple.* ACM Trans. Graphics 33/4 (2014), #70,1–9.

Seamless Surface Mappings

Yaron Lipman

(joint work with Noam Aigerman, Roi Poranne)

We introduce a method for computing seamless homeomorphic piecewise-linear (PL) mapping between two surface-meshes that interpolates a given set of point correspondences.

A common approach for computing a map between surfaces is to cut the surfaces to disks, flatten them to the plane, and extract the mapping from the flattenings by composing one flattening with the inverse of the other. So far, a significant drawback in this class of techniques is that the choice of cuts introduces a bias in the computation of the map that often causes visible artifacts and wrong correspondences.

In this work we develop a homeomorphic surface mapping technique that is indifferent to the particular cut choice. This is achieved by a novel type of PL surface flattening, named G-flattening that encodes this cut-invariance. Here, G denotes a sub-group of affine transformations in the plane. The key idea is to use an energy functional E that is invariant to compositions with transformations in G. This implies that the energy landscape of E does not change when the cuts are deformed homotopically on the surface. In turn, this implies that any map produced from G-flattenings is "blind" to the cut locations on the surfaces, up to a choice of homotopy class.

We present an algorithm based on these observations and demonstrate it is able to produce high-quality seamless homeomorphic mappings of pairs of surfaces exhibiting a wide range of shape variability, while using a small number of prescribed point correspondences. We also use this framework to produce three-way, consistent and seamless mappings for triplets of surfaces.

Polyhedra inscribed in a quadric and anti-de Sitter geometry

Jean-Marc Schlenker
(joint work with Jeffrey Danciger and Sara Maloni)

According to a celebrated result of Steinitz (see e.g. [13, Chapter 4]), a graph Γ is the 1–skeleton of a convex polyhedron in $\mathbb{R}^3$ if and only if Γ is planar and 3–connected. Steinitz [12] also discovered, however, that there exists a 3–connected planar graph which is not realized as the 1–skeleton of any polyhedron inscribed in the unit sphere S, answering a question asked by Steiner [11] in 1832. An understanding of which polyhedral types can or can not be inscribed in the sphere remained elusive until Hodgson, Rivin, and Smith [7] gave a computable but non-explict characterization in 1992, see below. Our first result is on realizability by polyhedra inscribed in other quadric surfaces in $\mathbb{R}^3$. Up to projective transformations, there are two such surfaces: the hyperboloid H, defined by $x_1^2+x_2^2-x_3^2=1$, and the cylinder C, defined by $x_1^2+x_2^2=1$ (with x_3 free).

Definition. A convex polyhedron P is *inscribed* in the hyperboloid H (resp. in the cylinder C) if $P \cap H$ (resp. $P \cap C$) is exactly the set of vertices of P.

Theorem A [3]. *Let Γ be a planar graph. Then the following conditions are equivalent:*

- *(C): Γ is the 1–skeleton of some convex polyhedron inscribed in the cylinder.*
- *(H): Γ is the 1–skeleton of some convex polyhedron inscribed in the hyperboloid.*
- *(S): Γ is the 1–skeleton of some convex polyhedron inscribed in the sphere and Γ admits a Hamiltonian cycle.*

The ball $x_1^2+x_2^2+x_3^2<1$ gives the projective model for hyperbolic space $\mathbb{H}^3$, with the sphere S describing the ideal boundary $\partial_\infty\mathbb{H}^3$. In this model, projective lines and planes intersecting the ball correspond to totally geodesic lines and planes in $\mathbb{H}^3$. Therefore a convex polyhedron inscribed in the sphere is naturally associated to a *convex ideal polyhedron* in the hyperbolic space $\mathbb{H}^3$.

Following the pioneering work of Andreev [1, 2], Rivin [8] gave a parameterization of the deformation space of such ideal polyhedra in terms of dihedral angles, as follows.

Theorem B (Andreev '70, Rivin '92). *The possible exterior dihedral angles of ideal hyperbolic polyhedra are the functions* $w : E(\Gamma) \to (0, \pi)$ *such that*

- *for each vertex* v*, the sum of the values of* w *on the edges adjacent to* v *is equal to* 2π*,*
- *for each other closed path* c *in the dual graph* Γ^**,* $\sum_{e \in c} w(e) > 2\pi$*.*

Each such function gives the angles of a unique ideal polyhedron in $\mathbb{H}^3$*.*

As a corollary, Hodgson, Rivin and Smith [7] showed that deciding whether a planar graph Γ may be realized as the 1–skeleton of a polyhedron inscribed in the sphere amounts to solving a linear programming problem on Γ. To prove Theorem A, we show that, given a Hamiltonian cycle in Γ, there is a similar linear programming problem whose solutions determine polyhedra inscribed in either the cylinder or the hyperboloid.

The solid hyperboloid $x_1^2 + x_2^2 - x_3^2 < 1$ in $\mathbb{R}^3$ gives a picture of the projective model for *anti-de Sitter* (AdS) geometry. Therefore a convex polyhedron inscribed in the hyperboloid is naturally associated to a convex ideal polyhedron in the anti-de Sitter space $\mathbb{AdS}^3$, which is a Lorentzian analogue of hyperbolic space. Similarly, the solid cylinder $x_1^2 + x_2^2 < 1$ (with x_3 free) in an affine chart $\mathbb{R}^3$ of $\mathbb{RP}^3$ gives the projective model for *half-pipe* (HP) geometry. Therefore a convex polyhedron inscribed in the cylinder is naturally associated to a convex ideal polyhedron in the half-pipe space $\mathbb{HP}^3$. Half-pipe geometry, introduced by Danciger [4, 5, 6], is a transitional geometry which, in a natural sense, is a limit of both hyperbolic and anti-de Sitter geometry.

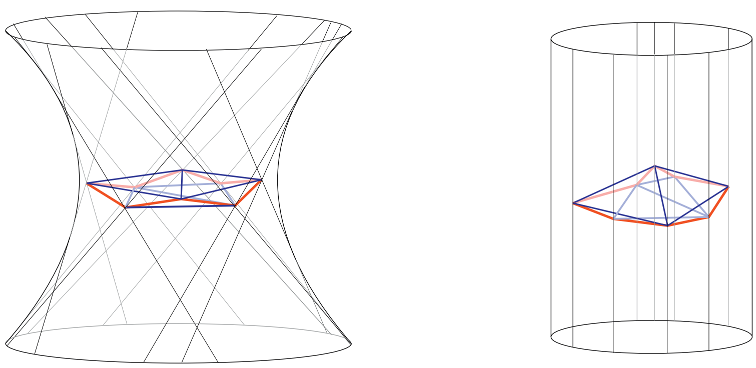

FIGURE 1. A polyhedron inscribed in the hyperboloid (left) and a combinatorial equivalent polyhedron inscribed in the cylinder (right). The 1–skeleton of any such polyhedron admits a Hamiltonian cycle which we call the *equator* (red/bold).

Theorem C [3]. *The possible exterior dihedral angles of ideal AdS polyhedra are the functions* $w : E(\Gamma) \to \mathbb{R}_{\neq 0}$ *such that*

- $w < 0$ *on a Hamiltonian cycle* γ, $w > 0$ *elsewhere,*
- *for each vertex* v*, the sum of the values of* w *on the edges adjacent to* v *is equal to* 0*,*
- *for each "other" closed path* c *in* Γ^**, crossing* γ *exactly twice, the sum of the values of* w *on the edges of* c *is strictly positive.*

Each such function gives the dihedral angles of a unique ideal polyhedron in $\mathbb{A}\mathrm{d}\mathbb{S}_3$*.*

The equivalence between conditions (H) and (S) in Theorem A follows from a direct argument comparing the conditions occuring in Theorem A and in Theorem C. For condition (C), one has to use instead of Theorem C its analog n half-pipe geometry.

Related results determine the possible induced metrics on ideal polyhedra. In the hyperbolic setting the following result is known.

Theorem D (Rivin '93). *Let* h *be a hyperbolic metric of finite area on* S^2 *with at least* 3 *cusps. There exists a unique ideal polyhedron* $\mathbb{H}^3$ *with induced metric* h *on its boundary.*

We have a similar result in the anti-de Sitter setting.

Theorem E [3]. *Let* h *be a hyperbolic metric of finite area on* S^2 *with at least* 3 *cusps, and let* γ *be a Hamiltonian cycle through the cusps. There exists a unique ideal polyhedron in* $\mathbb{A}\mathrm{d}\mathbb{S}_3$ *with induced metric* h *on its boundary and and equator* γ*.*

In spite of the close analogy between the hyperbolic and AdS statements, the proofs in the AdS case must be done along very different lines. The reason is that the hyperbolic proofs are largely based on the concavity of the volume of ideal hyperbolic polyhedra (in particular ideal simplices), while this property doesn't hold for ideal AdS polyhedra. Other arguments must therefore be developed.

There are a number of open questions stemming from those results on ideal AdS polyhedra. For instance, do the description of their dihedral angles and induced metrics extend to *hyperideal* AdS polyhedra, that is, polyhedra with all vertices *outside* $\mathbb{A}\mathrm{d}\mathbb{S}_3$ but all edges intersecting it? This basically happens in the hyperbolic setting [9, 10].

References

[1] E. M. Andreev, *Convex polyhedra in Lobačevskiĭ spaces*, Mat. Sb. (N.S.) **81 (123)** (1970), 445–478. MR 0259734 (41 #4367)

[2] ———, *Convex polyhedra of finite volume in Lobačevskiĭ space*, Mat. Sb. (N.S.) **83 (125)** (1970), 256–260. MR 0273510 (42 #8388)

[3] J. Danciger, S. Maloni, and J.-M. Schlenker, *Polyhedra inscribed in a quadric*, ArXiv e-prints (2014).

[4] Jeffrey Danciger, *Geometric transitions: From hyperbolic to AdS geometry.*, Ph.D. thesis, Stanford University, June 2011.

[5] ———, *A geometric transition from hyperbolic to anti-de Sitter geometry*, Geom. Topol. **17** (2013), no. 5, 3077–3134. MR 3190306
[6] ———, *Ideal triangulations and geometric transitions*, J. Topol., to appear (2014).
[7] Craig D. Hodgson, Igor Rivin, and Warren D. Smith, *A characterization of convex hyperbolic polyhedra and of convex polyhedra inscribed in the sphere*, Bull. Amer. Math. Soc. (N.S.) **27** (1992), no. 2, 246–251. MR 1149872 (93a:52009)
[8] Igor Rivin, *A characterization of ideal polyhedra in hyperbolic* 3*-space*, Ann. of Math. (2) **143** (1996), no. 1, 51–70. MR 1370757 (96i:52008)
[9] Jean-Marc Schlenker, *Métriques sur les polyèdres hyperboliques convexes*, J. Differential Geom. **48** (1998), no. 2, 323–405. MR 1630178 (2000a:52018)
[10] ———, *Convex polyhedra in Lorentzian space-forms*, Asian J. Math. **5** (2001), no. 2, 327–363. MR 1868937 (2003f:53127)
[11] Jakob Steiner, *Systematische entwickelung der abhängigkeit geometrischer gestalten von einander*, G. Fincke, 1832.
[12] Ernst Steinitz, *Über isoperimetrische probleme bei konvexen polyedern*, Journal für die reine und angewandte Mathematik **159** (1928), 133–143.
[13] Günter M. Ziegler, *Lectures on polytopes*, Graduate Texts in Mathematics, vol. 152, Springer-Verlag, New York, 1995. MR 1311028 (96a:52011)

Stripe patterns

Ulrich Pinkall
(joint work with Keenan Crane, Felix Knöppel, Peter Schröder)

This talk reports on recent results in [2] and how they are related to an earlier algorithm [1] concerning the approximation of velocity fields in space by fields that are generated by a collection of vortex filaments.

Many natural phenomena (animal skin, sand ripples...) exhibit stripe patterns on surfaces. We give an algorithm that generates such a pattern on a surface M based on the following data:

(1) An unoriented direction field defined away from finitely many points $p_1, \dots,$ $p_n \in M$ where the field fails to be orientable (i.e. to be representable by a continuous unit vector field in some neighborhood).
(2) A function $\rho : M \to \mathbb{R}_+$ that specifies the desired spacing of the stripes.

In the end the stripe pattern will be obtained in the form of a function $\alpha :$ $\tilde{M} - \{q_1, \dots, q_n\}$ where $\tilde{M}$ is the double cover of M branched over $p_1, \dots, p_n$. Here $q_1, \dots, q_n \in \tilde{M}$ are points (which include the branch points) where α might be discontinuous. So this is there we will find singularities of the stripe pattern.

Specifically, we find α in the form

$$\alpha = \arg \psi$$

where $\psi : \tilde{M} \to \mathbb{C}$ minimizes the energy

$$E(\psi) := \int_{\tilde{M}} |d\psi - i\omega\psi|^2$$

under the constraint $\int_M |\psi|^2 = 1$. Here ω is the 1-form on M that encodes the prescribed direction and spacing.

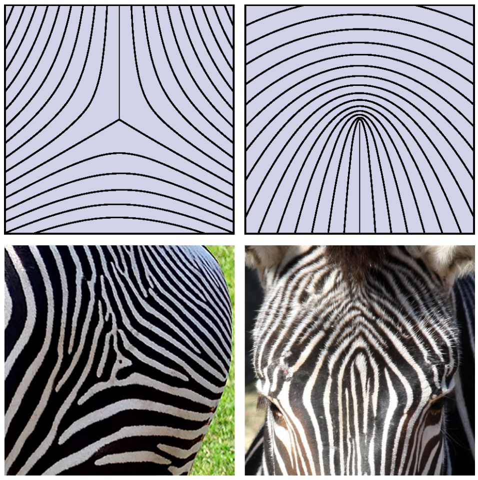

FIGURE 1. Stripe patterns in nature often exhibit nonorientable singularities.

The question in which sense the resulting stripe pattern realizes the prescribed data as closely as possible leads to non-trivial open problems concerning the statistical properties of the zeros of random sections of complex line bundles over surfaces.

References

[1] S. Weißmann and U. Pinkall and P. Schröder, *Smoke rings from smoke*, ACM Transactions on Graphics **33** (2014), 140:1–140:8.

[2] K. Crane and F. Knöppel and U. Pinkall and P. Schröder, *Stripe patterns on surfaces*, to appear in ACM Transactions on Graphics (Siggraph 2015).

Fast and Exact (Poisson) Solvers on Surfaces of Revolution

MICHAEL KAZHDAN

We consider the problem of solving Poisson-like systems on surfaces of revolution. On the one hand, these geometries contain sufficient regularity to enable the design of an efficient exact solver. On the other, they include surfaces with varying curvature – so an efficient solver makes it possible to interactively explore how the surface metric interacts with the Laplace-Beltrami operator.

The key to our approach derives from the observation that isometry invariant operator must commute with the symmetry group of the geometry, and hence the linear operator becomes block-diagonal in the irreducible representations of the group, with (at least) one block associated with each class of irreducible representations. Thus, rather than having to solve one large linear system of equations, we obtain the solution to the linear system by solving multiple smaller ones.

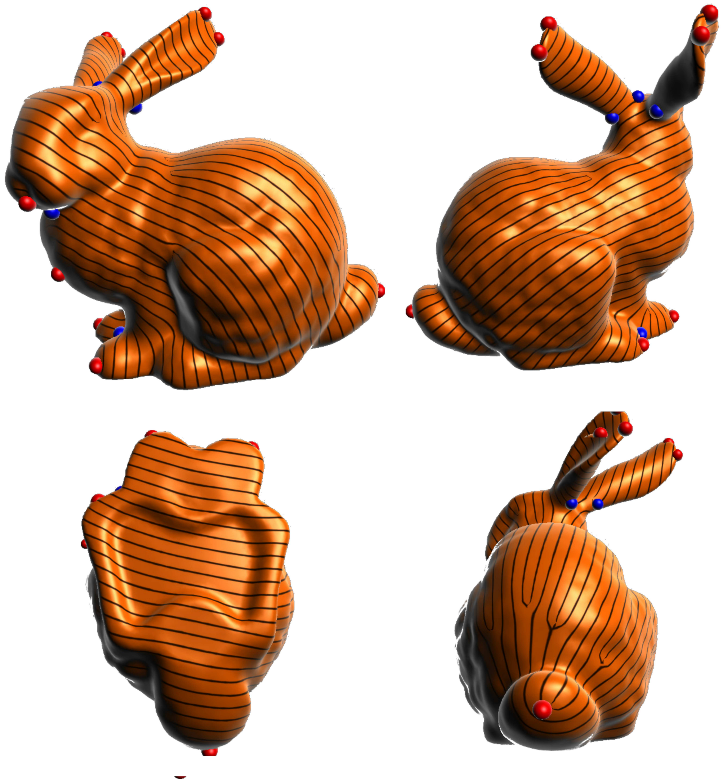

FIGURE 2. A stripe pattern with constant prescribed spacing. Note the additional singularities that are generated by the algorithm.

In the particular case of a surface of revolution, sampled on an $N \times N$ grid, this implies that when the linear operator commutes with the cyclic group we can solve the $N^2 \times N^2$ system by solving N different sub-systems, each of size $N \times N$. Furthermore, we show that if the linear operator also commutes with the dihedral group, then the same approach extends to surfaces with boundary, obtained by sweeping the generating curve by an angle $< 360°$ about the axis of revolution.

This generalizes the approach proposed by Hockney [Hoc65] for solving the discrete Poisson equation in the plane to the solution of general linear systems on surfaces of revolution that commute with rotation about the axis of revolution. It also extends earlier methods for block-circulant systems [Dav79, BB06] to more general groups.

Representation Theoretic Perspective. We begin by recalling a basic theorem from representation theory ([Ser77, FH91]).

Theorem (Canonical Decomposition)**.** *Given a representation ρ of a finite/compact group G onto a vector space V, the vector space can be decomposed as the direct sum of irreducible representations, with multiplicity:*

$$V = \bigoplus_{\omega\in\Omega} V^\omega \qquad \text{with} \qquad V^\omega = \bigoplus_{k=1}^{m_\omega} V_k^\omega$$

where V_k^ω are irreducible representations, m_ω are the multiplicitices, and $V_k^\omega \approx V_{\tilde{k}}^{\tilde{\omega}}$ iff. $\omega = \tilde{\omega}$.

Using the uniqueness of the decomposition, it follows (by Schur's Lemma and Maschke's Theorem) that:

Lemma 1. *Given a representation (ρ, V) of a group G, if L is a G-linear map then $L(V^\omega) \subset V^\omega$ for all ω.*

Corollary 1. *If L is G-linear and $\{v_1^\omega, \dots, v_{d_\omega}^\omega\}$ is a basis for V^ω, then L is block diagonal in the basis $\{v_1^\omega, \dots, v_{d_\omega}^\omega\}_{\omega\in\Omega}$. In particular, solving the system $Lx = b$ can be done by solving $|\Omega|$ systems each of size $d_\omega \times d_\omega$, rather than solving a single system of size $\sum d_\omega \times \sum d_\omega$.*

Without loss of generality, we will assume that $V = V^\omega$ and write $V = \bigoplus_{k=1}^m V_k$ where the $V_i \approx V_j$. We set n to the dimension of V_k and we set $\iota_k : V_1 \to V_k$ to the isomorphism between the irreducible representations.

Definition We say that a basis $\{v_j^k\}_{(j,k)\in[1,m]\times[1,n]}$ with $v_j^k \in V_k$ is *consistent* if $v_j^k = \iota_k(v_j^k)$.

It is not hard to show that as G becomes more complicated (and irreducible representations are no longer one-dimensional) there is further opportunity to take advantage of symmetry in designing an efficient solver:

Lemma 2. *If V is a complex vector space and $L : V \to V$ is G-linear, then the matrix representation of L in a consistent basis consists of $m \times m$ blocks where each block is a multiple of the identity.*

Corollary 2. *If we choose a consistent basis, then each dim$(V^\omega) \times$ dim(V^ω) block of the matrix representation of L further decomposes into a block diagonal matrix with dim(V_1^ω)* identical *blocks, each of size $m_\omega \times m_\omega$.*

Implications for Surfaces of Revolution (Sampled on an $N \times N$ Grid). The above discussion has immediate implications for solving linear systems over surfaces of revolution.

Rotations: Taking $G = C_N$ to be the cyclic group, we obtain a decomposition of the space of functions on the surface of revolution $\mathcal{F}$ with respect to the irreducible representations of G:

$$\mathcal{F} = \bigoplus_{\omega=-N/2}^{N/2} \mathcal{F}_C^\omega$$

where $\mathcal{F}_C^\omega$ is the space of functions which, restricted to any parallel of the surface of revolution, are complex exponentials of frequency ω.

By Corollary 1 it follows that if L is G-linear, there exist linear operators $\{L^\omega : \mathcal{F}_C^\omega \to \mathcal{F}_C^\omega\}_{|\omega|\leqslant N/2}$ such that if $f = \sum_\omega f^\omega$, with $f^\omega \in \mathcal{F}_C^\omega$ then:

$$L(f) = \sum_{\omega=-N/2}^{N/2} L^\omega(f^\omega).$$

Rotations + Reflections: Taking $G = D_{2N}$ to be the dihedral group, we obtain a decomposition of the space of functions on the surface of revolution $\mathcal{F}$ with respect to the irreducible representations of G:

$$\mathcal{F} = \bigoplus_{\omega=0}^{N/2} \mathcal{F}_D^\omega \qquad \text{with} \qquad \mathcal{F}_D^\omega = \mathcal{F}_D^{\omega+} \oplus \mathcal{F}_D^{\omega-}$$

where $\mathcal{F}_D^{\omega+}$ (respectively $\mathcal{F}_D^{\omega-}$) is the space of functions which, restricted to any parallel of the surface of revolution, are multiples of the cosine (respectively sine) functions of frequency ω.

By Corollary 2 it follows that if L is G-linear, there exist linear operators $\{L^\omega : \mathcal{F}_D^{\omega\pm} \to \mathcal{F}_D^{\omega\pm}\}_{0\leqslant\omega\leqslant N/2}$ such that if $f = \sum_\omega f^\omega$, with $f^\omega \in \mathcal{F}_D^{\omega+}$ (respectively $f^\omega \in \mathcal{F}_D^{\omega-}$) then:

$$L(f) = \sum_{\omega=0}^{N/2} L^\omega(f^\omega).$$

Surfaces of Revolution with Boundaries. We can extend the results for surfaces of revolution to surfaces of revolution with boundary, obtained by rotating a generating curve by angle $< 360°$, despite the fact that there is no group action. Specifically, taking a double-covering of the surface with boundary, where we attach a second copy of the domain at the angular boundaries, we obtain a surface of revolution on which we have an action of D_{4N}.

Decomposing the space of functions on the double-covering into even/odd functions (functions which have the same/negative values on the two pre-images of a point), we can associate these with the spaces of functions on the initial surface with boundary satisfying Neumann/Dirichlet constraints. Thus, if L is a linear operator on the double-covering that commutes with the action of D_{4N}, it follows that it will map the even/odd subspaces back into themselves, giving a block diagonalization of the corresponding linear operator on the surface with boundary.

Applications. Incorporating our solver in systems performing wave simulation using implicit time integration, we are able to process signals on high-resolution surfaces of revolution (with boundary) at interactive rates. For example, sampling such a surface at resolution $N \times N = 1024 \times 1024$, we can solve the system of equations with roughly one million unknowns at a rate of 20 frames-per-second, significantly outperforming both the running time and memory usage of standard solvers [CDHR08].

References

[BB06] Bindel D., Bruyns C.: Shape-changing symmetric objects for sound synthesis. In *Audio Engineering Society 121* (2006), pp. 875–881.

[CDHR08] Chen Y., Davis T., Hager W., Rajamanickam S.: Algorithm 887: Cholmod, supernodal sparse Cholesky factorization and update/downdate. *ACM Transactions on Mathematical Software 35*, 3 (2008), 22:1–22:14.

[Dav79] Davis P.: *Circulant matrices.* Pure and applied mathematics. Wiley, 1979.

[FH91] Fulton W., Harris J.: *Representation Theory: A First Course.* Springer-Verlag, New York, 1991.

[Hoc65] Hockney R.: A fast direct solution of Poisson's equation using Fourier analysis. *Journal of the ACM 12*, 1 (1965), 95–113.

[Ser77] Serre J.: *Linear representations of finite groups.* Springer-Verlag, New York, 1977.

Approximating Curved Surfaces with Miura-Ori Origami

Etienne Vouga

(joint work with L. Dudte, L. Mahadevan)

Because of their simplicity and geometric properties, origami tessellations – particularly those generated by folding along creases that tile the plane periodically, such as the Miuri-ori pattern formed by tiling the plane with a unit cell of four congruent parallelograms – are highly suitable for engineering deployable or foldable structures. The Miura pattern in particular has four important geometric properties, in addition to its high degree of symmetry: *(a)* it can be *rigidly folded* isotopically from its flat, planar state to a folded state; *(b)* has only one isometric degree of freedom, with the shape of the entire structure determined by the folding angle of any single crease; *(c)* exhibits negative Poisson's ratio: folding the Miura decreases its extent in both planar directions; and *(d)* is *flat-foldable*: when the Miura has been maximally folded along its one degree of freedom, all faces of the pattern are coplanar.

Given an arbitrary surface with intrinsic curvature, does there exist a Miura-like tessellation of the plane that, when folded, approximates that surface? Can this pattern be made rigidly foldable with one degree of freedom? Building on the existing mathematics of rigid foldability, the mechanics of folded structures, and existing exploration of the *forward* problem of how modifying the pattern modifies the folded geometry [1, 2], we demonstrate that the inverse problem of fitting Miura-like origami tessellations to surface with intrinsic curvature can be solved for a large variety of such surfaces.

The simplest case is that of generalized cylinders – developable surfaces formed by extruding a planar curve along the perpendicular axis. For such surfaces an explicit construction exists for how to approximate them using a modified Miura tessellation, and moreover, it can be shown that the constructed pattern is rigid-foldable. For doubly-curved surfaces, Miura patterns can be found computationally to fit the surface; our experiments with this tool reveal that the space of possible Miura designs is extremely rich, with most surfaces admitting many different Miura approximations. While the Miura tessellations found using our tools

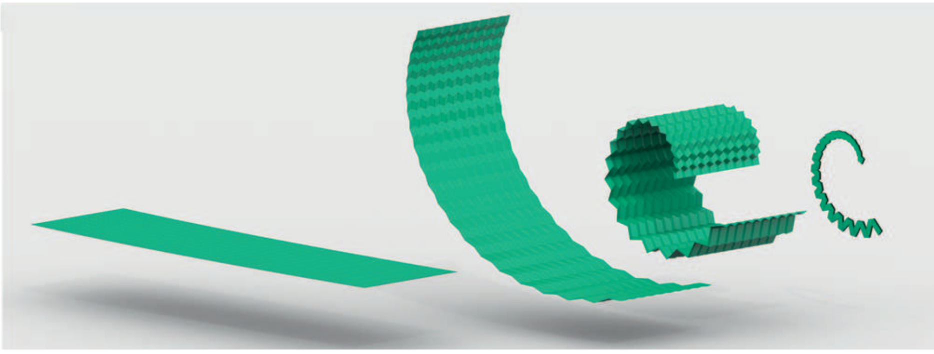

Figure 1. A Miura pattern approximating a generalized cylinder: the planar fold pattern (left) folds isotopically with one degree of freedom to the target shape (middle-right) and, since the pattern is flat-foldable, to a flat fully-folded configuration (right).

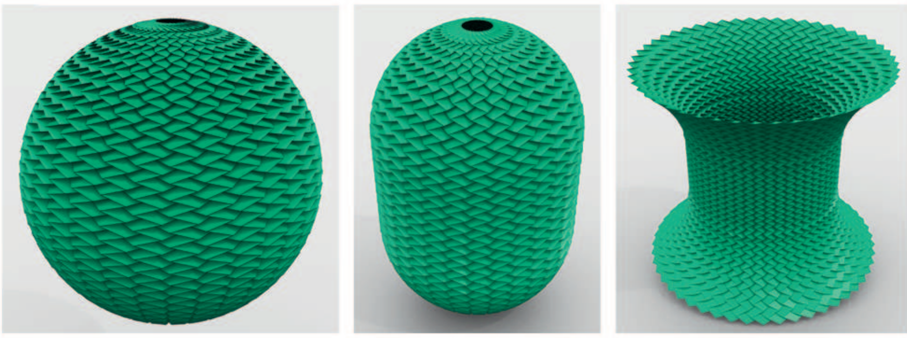

Figure 2. Some example generalized Miura patterns, generated using numerical optimization, approximating curved surfaces.

are not necessarily flat-foldable, with suitable modification of the optimization process, the strain needed to fold the pattern can be reduced.

Geometry of the Miura

It is clear that the space of shapes that can be approximated by perfectly periodic tilings of the plane is very limited. We therefore study Miura-like generalized origami tessellations, whose unit cells are not necessarily congruent but vary smoothly in shape across the tessellation. An embedding of such a pattern in space can be represented as a quadrilateral mesh: a set of vertices; edges connecting the vertices and representing the pattern creases; and faces, with exactly four faces meeting at each interior vertex. A quadrilateral mesh of regular valence four must satisfy two additional constraints to be an embedding of a generalized Miura tessellation: each face must be planar, and the neighborhood of each vertex must be *developable*, i.e. the interior angles around that vertex must sum to 2π.

A generalized Miura tessellation is guaranteed to possess some, but not all, of the four geometric properties of the regular Miura pattern. A unit cell in general position has only one degree of freedom, and this local property guarantees that the Miura pattern, if it is rigid-foldable at all, must have only one degree of freedom. Moreover, since each unit cell must consist of three valley and one mountain crease, or vice-verse, it must fold with negative Poison's ratio. That leaves flat- and rigid-foldability. Unfortunately, no local condition is known for whether an origami pattern is flat-foldable, and it has been shown [3] that the problem of determining flat-foldability is NP-complete. However, several necessary flat-foldability conditions do exist, including Kawasaki's Theorem that if a generalized Miura tessellation is flat-foldable, each pair of opposite interior angles around each vertex must sum to π. In practice, enforcing Kawasaki's theorem does improve the degree to which a generalized Miura tessellation is flat-foldable. Finally, a non-trivial flat-foldable generalized Miura is always rigid-foldable [1], and in the case where a flat-foldable configuration cannot be found, one can characterize the degree of non-rigid-foldability by measuring the maximum strain required to snap the tessellation through from its flat to its embedded state.

Curvilinear Miura Patterns

For arbitrary curved surfaces, fitting a generalized Miura pattern is a difficult nonlinear optimization problem, with convergence far from guaranteed absent a good initial guess for how the pattern should be laid out. An alternative to brute-force optimization is suggested by the following observations: 1) the edges of the generalized Miura fold pattern can be grouped into eight equivalence classes, corresponding to the eight fold lines that make up a unit cell. Edges in each equivalence class vary smoothly over the surface, suggestive of a discrete vector field on the surface; 2) generalized Miura patterns come in scale-invariant families, with corresponding edges in two members of the family nearly parallel and uniformly scaled. A Miura pattern approximating a surface M can thus be specified *on the surface* M by eight vector fields u^i, a scalar thickness field η, and a length scale ϵ. From a starting point $p \in M$, the first vertex of the Miura pattern is at $p + \eta\epsilon\hat{n}(p)$, where $\hat{n}$ is the surface normal. To get the second point, flow along u^0 for time ϵ to get a new "base point" $p^0 \in M$, then place a vertex at $p^0 - \eta\epsilon\hat{n}(p^0)$. By continuing in this way, alternating which vector field is used for the flow, and choosing the sign of the normal displacement appropriately, the entire pattern can be constructed. The pattern is valid if all faces are planar, and if all vertices have zero angle deficit; analyzing these constraints for finite ϵ is intractable, but in the limit of an *infintesimal* Miura pattern, when $\epsilon \to 0$, satisfying the constraints to first-order in ϵ can be expressed in terms of u^i, η, and the surface metric and curvatures. In the special case of ruled surfaces, the faces of the generalized Miura pattern can be made parallelograms, greatly simplifying these equations and allowing a direct construction where the vector fields u^i follow ruling and curvature lines;

the general case for positively-curved surfaces remains open, though naive degree-counting and numerical evidence using optimization tools suggest such patterns should exist.

References

[1] T. Tachi, *Generalization of Rigid Foldable Quadrilateral Mesh Origami*, Proceedings of the International Association for Shell and Spatial Structures (2009).
[2] M. Gattas and Z. You, *Miura-Base Rigid Origami: Parametrizations of Curved-Crease Geometries*, J. Mech. Des. **136** (2014).
[3] M. W. Bern and B. Hayes, *The Complexity of Flat Origami*, Proceedings of the Seventh Annual ACM-SIAM Symposium on Discrete Algorithms (1996), 175–183.

Strict minimizers

Denis Zorin
(joint work with Zohar Levi)

A variety of problems in geometry processing are solved by minimizing a global measure of distortion over a surface or volume. For example, computing the deformation of an object to a new pose can be achieved by setting a few target locations to new positions and minimizing a measure of isometric distortion; parameterizing a surface, or computing surface-to-surface map via an intermediate domain may be done by computing a pair of maps minimizing deviation from conformality.

In most cases, the global functional is obtained by making two choices: (1) *a local*, pointwise measure of distortion (for example, deviation from isometry or quasiconformal distortion); (2) a way to aggregate pointwise distortion into a single scalar measuring global distortion.

The second choice determines how distortion is distributed on the surface. L_2-norm of the distortion, viewed as a function on the surface emphasizes the decrease in average distortion, but allows arbitrarily high local distortion. On the opposite end of the spectrum, L_∞-norm ensures the tightest possible control on the worst-case distortion. Unfortunately, it does not, in general, yield a unique solution. Moreover, below the maximal distortion, it does not distinguish between solutions with just one or all elements (triangles or tets) with high distortion. We describe a different approach of controlling distortion distribution. We use the notion of *strict minimizers* that appeared in a variety of contexts, in particluar in economics as one of possible models of fairness; these minimizers do not correspond to a globally defined energy. Rather, they are minimal with respect to an ordering of pointwise distortion distributions on a surface. Computing strict minimizers using a precise algorithm that follows the definition can be impractically expensive. We introduce two approximate algorithms representing different accuracy-performance tradeoffs.

The algorithms are applicable to a number of applications, such as deformation, surface-to-surface mapping, and shape interpolation.

This work is described in [1].

References

[1] Z. Levi, D. Zorin, *Strict minimizers for geometry optimization*, ACM Transactions on Computer Graphics **33**, 6 (2014), 185

Nested Cages

Alec Jacobson

(joint work with Leonardo Sacht, Etienne Vouga)

Many tasks in geometry processing and physical simulation benefit from multiresolution hierarchies: efficient PDE solving, collision detection culling, physically based simulation, and cage-based geometric modeling. As a motivating example, consider solving a Poisson equation $\mathbf{Ax} = \mathbf{b}$ via finite-element method inside a non-convex subregion $\Omega \in \mathbb{R}^3$ approximated by 7M-tetrahedra mesh. In-core direct solvers are out of the question when memory is limited. Multiresolution solves this problem efficiently with the following recursive algorithm[1] operating over a sequence of progressively coarser mesh approximations of the domain:

(1) *Relax* initial guess $\mathbf{x}$ according to $\mathbf{A}$,
(2) Compute residual $\mathbf{r} = \mathbf{Ax} - \mathbf{b}$,
(3) *Restrict* residual from fine mesh to coarser mesh $\mathbf{r}_c = \mathbf{P}^\mathsf{T}\mathbf{r}$,
(4) *Solve* $\mathbf{A}_c\mathbf{u}_c = \mathbf{r}_c$ for "update" *on* coarser mesh,
(5) *Prolongate* "update" and add to running guess $\mathbf{x} \leftarrow \mathbf{x} + \mathbf{Pu}_c$,
(6) *Relax* $\mathbf{x}$ according to $\mathbf{A}$,

where *Relax* typically means applying a few Jacobi or Gauss-Seidel iterations, *Restrict* approximates a function defined on fine mesh vertices by one on coarse mesh vertices, *Solve* applies these six steps recursively, and *Prolongate* takes a function back up to the fine mesh. If the fine-mesh vertices lie strictly inside the coarse mesh, then the $\mathbf{P}$ is simple linear interpolation. To ensure that equations on coarser levels faithfully approximate lower frequencies of the original problem, meshes should have the same topology and similar geometry.

Existing techniques such as surface mesh decimation, voxelization, or contouring distance level sets, violate one or more of three characterstics: strict nesting, homeomorphic topology and geometric closeness. Instead, our methods successively constructs each next-coarsest level of the hierarchy, using a sequence of decimation, flow, and contact-aware optimization steps. From coarse to fine, each layer then fully *encages* the next while retaining a snug fit and respecting the original surface topology.

The input to our method is a sequence of decimations of the original mesh which match its topology, but, in general, overlap. The output is a new embedding for each mesh (i.e. new vertex positions) such that each tightly contains all finer meshes. Our approach works pairwise, from the finest layer to coarsest. Each inductively contains all finer layers.

[1] Known as "rediscretization multiresolution" as opposed to "Galerkin multiresolution" which is intractable on unstructured hierarchies in $\mathbb{R}^3$.

The pairwise problem is broken down into two stages: flow the fine mesh inside the coarse mesh and then *re-inflate* the fine mesh to its original position while *pushing* the coarse mesh outward.

Flow To attract the fine mesh F inside the coarse mesh $\widehat{C}$ we flow it opposite the gradient of an energy integrating signed distance to the coarse mesh. In the continuous setting we write this as:

$$\Phi(\bar{\mathbf{F}}) = \int_F s(\bar{\mathbf{p}}) d(\bar{\mathbf{p}})\, dA, \longrightarrow \frac{\partial \bar{\mathbf{f}}}{\partial t} = -\nabla_{\bar{\mathbf{f}}} \Phi(\bar{\mathbf{F}}), \tag{1}$$

where $\bar{\mathbf{p}}$ is a point on the fine mesh, s and d compute the sign (1 outside, -1 inside) and distance to the coarse mesh.

This flow is non-trivial to discretize. We first approximate the integral with higher-order quadrature points sampled inside fine mesh facets. Then we employ a technique common to surface registration. During each small step of the flow, for each point $\bar{\mathbf{p}}$ we *freeze* its associated closest point on $\widehat{C}$, therefore linearizing its signed distance gradient direction. We continue along this flow until the fine mesh is full inside the coarse mesh. In contrast to normal flows, this flow guides the fine mesh toward the medial axis of the coarse mesh.

Re-inflation Next we reverse the flow, marching the fine mesh back along its path, but now we resolve collisions with the coarse mesh *à la* physically based simulation. There are many feasible embeddings for the coarse mesh so we regularize, treating the problem as a constrained optimization:

$$\min_{\mathbf{C}} E(\mathbf{C}) \text{ subject to: } C \text{ does not intersect itself or } \bar{F}. \tag{2}$$

In physics parlance, we find a static solution for each reverse time step as $\bar{F}$ moves like an infinite mass obstacle toward its original position and pushes the deformable C outward.

We leverage state-of-the-art physically-based simulation contact mechanics methods to satisfy these constraints. There are a variety of reasonable choices for E: total volume, total displacement, surface deformation, volumetric deformation.

This pairwise method operates iteratively to create sequences of strictly nested, yet tightly fitting cages. We demonstrate the effectiveness of these cages for: improving convergence of geometric multiresolution (especially for Neumann boundary conditions), improving collision culling (especially for very non-convex shapes), and enabling cage construction for simulation and cage-based deformation where detailed shapes are embedded inside a deforming coarse cage.

Our heuristic is only a first step toward solving a very difficult problem. It is easy to find impossible cases (where no embedding of the coarse mesh will strictly nest a given fine mesh), but a general test of feasibility is elusive, much less an algorithm with strong guarantees of success. We excitedly look forward to improving upon our method by considering optimizing all layers simultaneously. We would also like to analyze our multiresolution solver and determine whether there exists a concept of "nested enough." Finally, we would like to apply our multiresolution hierarchies to more complicated, harder problems: quadratic programs and second-order conic programs.

References

[1] T. Chan, S. Go, J. Zou, *Boundary treatments for multilevel methods on unstructured meshes*, SIAM Journal on Scientific Computing (1999).

On the Blaschke-Bol problem in the plane

Fedor Nilov

We find several essentially new constructions of hexagonal 3-webs based on a combination of quadratic and linear families of circles. They are used to construct 5 new types of hexagonal 3-webs, which is an advance in the solution of the Blaschke-Bol problem (1938) on the classification of such webs. Unlike many known examples, in our proofs we give an explicit parallelizing diffeomorphism. We give a brief survey of all known examples of hexagonal 3-webs and their properties. In conclusion, we formulate several conjectures and open problems.

The circumcenter of mass

Serge Tabachnikov

This talk is a survey of the recent work on an interesting geometrical construction, the *circumcenter of mass* [8, 3].

Consider a plane polygon P. Triangulate it, and assign the circumcenter to each triangle of the triangulation. Take these points with the weights equal to the (signed) areas of the respective triangles, and consider the center of mass of this system of point-masses. This center of mass does not depend on the triangulation; this is the circumcenter of mass of P, denoted by $CCM(P)$.

This construction resembles that of the center of mass, $CM(P)$, of a polygonal lamina P. That the result does not depend on the triangulation, follows from the Archimedes Lemma: if an object is divided into two smaller objects, then the center of mass of the compound is the weighted sum of the centers of mass of the two smaller objects. The same applies to $CCM(P)$.

This construction is not new. In [5], it is attributed to an Italian algebraic geometer G. Bellavitis. It was rediscovered by V. Adler as an integral of his polygon recutting transformation [1, 2] and, independently, by B. Grünbaum and G. Shephard [4]. It is also an integral of the discrete bicycle transformation [7], a.k.a. a discrete analog of the smoke ring flow [6].

Here are some properties of $CCM(P)$:

- if P is an equilateral polygon then $CCM(P) = CM(P)$;
- the continuous limits of $CCM(P)$ and $CM(P)$ coincide;

- if a 'center' is assigned to every polygon such that it commutes with dilations, satisfies the Archimedes Lemma, and depends analytically on the polygon, then it is an affine combination of $CCM(P)$ and $CM(P)$.

The construction extends to simplicial polytopes in higher dimensions. The following result is due to A. Akopyan: if the sums of squared edge lengths of all facets of P are the same then $CCM(P) = CM(P)$. One can also extend the construction to the spherical and hyperbolic geometries.

In search of an axiomatic approach, one has the following result, see [9]: assign to every non-degenerate simplex Δ a 'center' $C(\Delta)$ so that:

(1) The map $\Delta \mapsto C(\Delta)$ commutes with similarities;
(2) The map $\Delta \mapsto C(\Delta)$ is invariant under the permutations of the vertices of the simplex Δ;
(3) The map $\Delta \mapsto \mathrm{Vol}(\Delta)C(\Delta)$ is polynomial in the coordinates of the vertices of the simplex Δ.

Then $C(\Delta)$ is an affine combination of the center of mass and the circumcenter:

$$C(\Delta) = tCM(\Delta) + (1-t)CCM(\Delta),$$

where the constant t depends on the map $\Delta \mapsto C(\Delta)$ (and not on the simplex Δ).

References

[1] V. Adler, *Cutting of polygons.* Funct. Anal. Appl. **27** (1993), 141–143.
[2] V. Adler, *Integrable deformations of a polygon.* Phys. D **87** (1995), 52–57.
[3] A. Akopyan, *Some remarks on the circumcenter of mass.* Discrete Comput. Geom. **51** (2014), 837–841.
[4] B. Grünbaum. Private communication.
[5] C.-A. Laisant, *Théorie et applications des équipollences.* Gauthier-Villars, Paris 1887, pp. 150–151.
[6] U. Pinkall, B. Springborn, S. Weissmann, *A new doubly discrete analogue of smoke ring flow and the real time simulation of fluid flow.* J. Phys. A **40** (2007), 12563–12576.
[7] S. Tabachnikov, E. Tsukerman, *On the discrete bicycle transformation.* Publ. Math. Uruguay (Proc. Montevideo Dynam. Syst. Congress 2012) **14** (2013), 201–220
[8] S. Tabachnikov, E. Tsukerman, *Circumcenter of Mass and generalized Euler line.* Discr. Comp. Geom. **51** (2014), 815–836.
[9] S. Tabachnikov, E. Tsukerman, *Remarks on the circumcenter of mass.* arXiv:1410.5115.

Grassmann Orbitopes

Raman Sanyal

An *orbitope* is the convex hull of the orbit of a point under the action of a compact group. This particular class of highly symmetric convex bodies was explored in collaboration with Frank Sottile and Bernd Sturmfels [5]. With the additional assumption that the group G is algebraic and the linear action of G on the ambient real vector space V is rational, the orbit $G \cdot v$ for $v \in V$ is a real-algebraic variety and the orbitope $\mathcal{O}_v = \mathrm{conv}(G \cdot v)$ is a semi-algebraic set. Thus orbitopes are prime examples of the field *convex algebraic geometry*, the intersection of convex geometry, real-algebraic geometry, and optimization.

If G is finite, then $\mathcal{O}_v$ is a convex polytope. This very general construction yields many well-known polytopes, including the regular solids. A particular class of examples are the generalized permutahedra: For a point $\lambda = (\lambda_1, \ldots, \lambda_d) \in \mathbb{R}^d$, the *generalized permutahedron* is the polytope

$$\Pi(\lambda) \; = \; \mathrm{conv}\{(\lambda_{\sigma(1)}, \ldots, \lambda_{\sigma(d)}) : \sigma \text{ permutation}\}.$$

Generalized permutahedra occur in many areas including geometric combinatorics, representation theory, and algebraic geometry.

For general groups G, orbitopes $\mathcal{O}_v$ are typically proper convex bodies with infinitely many extreme points. An interesting class of examples are the Schur-Horn orbitopes that yield a continuous generalization of permutahedra: Let $G = O(d)$ be the orthogonal group acting on real $d \times d$-matrices $\mathrm{Sym}_2\mathbb{R}^d$ by conjugation, that is, $g \cdot B := gAg^t$ for $g \in G$ and $B \in \mathrm{Sym}_2\mathbb{R}^d$. For a symmetric matrix B, we write $\lambda(B) = (\lambda_1 \geqslant \lambda_2 \geqslant \cdots \geqslant \lambda_d)$ for its vector of real eigenvalues. For $A \in \mathrm{Sym}_2\mathbb{R}^d$, the orbit $G \cdot A$ is the collection of symmetric matrices B with $\lambda(B) = \lambda(A)$. The *Schur-Horn orbitope* is $\mathcal{S}(A) := \mathrm{conv}(G \cdot A)$. There are many striking similarities between permutahedra and Schur-Horn orbitopes (see [5, Sect. 3]) most of which are a result of the following application of the well-known Schur-Horn theorem: Let us denote by $\pi : \mathrm{Sym}_2\mathbb{R}^d \to \mathbb{R}^d$ the linear projection onto the diagonal. Then the following holds

$$\pi(S(A)) \; = \; \Pi(\lambda(A)).$$

A class of convex bodies that is computational tractable is that of spectrahedra. A *spectrahedron* is an affine section of the cone of semidefinite matrices (also known as the PSD-cone). Equivalently, a spectrahedron is a set of the form

$$S \; = \; \{x \in \mathbb{R}^d : A_0 + x_1A_1 + \cdots + x_dA_d \text{ positive semidefinite}\}$$

for some symmetric matrices $A_0, \ldots, A_d$. Spectrahedra are exactly the feasible regions of semidefinite programs, a powerful extension of linear programming. Choosing all A_i diagonal yields the usual definition of polyhedra. In [5] we show that the Schur-Horn orbitopes are spectrahedra.

Interesting and important in differential geometry are the Grassmann orbitopes. Let $V = \wedge^k\mathbb{R}^n$ be the k-th exterior power of $\mathbb{R}^n$. The standard action of $G = O(n)$ on $\mathbb{R}^n$ induces an action on V. For $v = e_1 \wedge e_2 \wedge \cdots \wedge e_n$, the points of the orbit $\mathrm{G}_{k,n} := G \cdot v$ are in bijection with oriented k-dimensional linear subspaces of $\mathbb{R}^n$. The *Grassmann orbitope* (or *mass ball*) is defined as $\mathcal{G}_{k,n} := \mathrm{conv}(\mathrm{G}_{k,n})$. An *exposed face* of $\mathcal{G}_{k,n}$ is the set of points maximizing a linear function ℓ over $\mathcal{G}_{k,n}$. If the maximal value of ℓ over $\mathcal{G}_{k,n}$ is 1, then ℓ is called a *calibration.* According to the Fundamental Theorem of Calibrations [2], calibrations give certificates for manifolds to be area minimizing with given boundary. The points $\mathrm{G}_{k,n} \cap \{\ell = 1\}$ are the *calibrated geometries.*

For $k \in \{1, n-1\}$, the Grassmann orbitopes are just n-dimensional balls B_n. The Grassmann orbitope $\mathcal{G}_{2,4}$ is linearly isomorphic to $B_3 \times B_3$. For $k \in \{2, n-2\}$, the Grassmann orbitopes are skew-symmetric versions of the Schur-Horn orbitopes and hence spectrahedra. This implies that calibrated geometries and calibrations can be explored experimentally using the standard software for semidefinite programming.

For $2 < k < n-2$, our knowledge of the faces of $\mathcal{G}_{k,n}$ is very scarce. The Grassmann orbitope $\mathcal{G}_{3,6}$ was described by Dadok and Harvey [1] and Morgan [4]. The results were extended to $\mathcal{G}_{3,7}$ by Harvey and Morgan [3]. It can be shown that these Grassmann orbitopes are not spectrahedra.

In joint work with Philipp Rostalski, we used state-of-the-art methods from polynomial optimization to explore Grassmann orbitopes *computationally*. The basic idea is the following: Maximizing a linear function ℓ over $\mathcal{G}_{k,n}$ is equivalent to finding the minimal δ such that $\delta - \ell(p) \geqslant 0$ for all $p \in G \cdot v$. It is in general difficult to assert that a (linear) function $\delta - \ell$ is nonnegative. A tractable relaxation is to replace it with the weaker condition of being a sum-of-squares: find the minimal δ such that

$$(1) \qquad \delta - \ell(p) \;=\; h_1(p)^2 + h_2(p)^2 + \cdots + h_m(p)^2 \qquad \text{for all } p \in \mathrm{G}_{k,n}$$

for some polynomials $h_1, \ldots, h_m$. The Grassmannian $\mathrm{G}_{k,n}$ is a compact real variety with vanishing ideal $I_{k,n} \subset \mathbb{R}[p_I : I \subseteq [n], |I| = k]$ consisting of the Plücker relations plus the equation of the unit sphere. Hence, (1) is equivalent to the condition that $\delta - \ell - \sum_i h_i^2 \in I_{k,n}$. For an upper bound D on the degree of the polynomials h_i, the relaxed optimization problem can be cast into a semidefinite programming problem. This is computationally tractable if D is small. For $n \leqslant 7$, we found that $D = 1$ suffices. That is, every calibration is a sum-of-squares of linear polynomials relative to $I_{k,n}$. We conjecture that this holds true for all Grassmann orbitopes. It turns out that our conjecture is equivalent to a question of Harvey and Lawson [2, Question 6.5].

References

[1] Jiri Dadok and Reese Harvey, *Calibrations on* $\mathbf{R}^6$, Duke Math. J. **50** (1983), no. 4, 1231–1243.

[2] Reese Harvey and H. Blaine Lawson, Jr., *Calibrated geometries*, Acta Math. **148** (1982), 47–157.

[3] Reese Harvey and Frank Morgan, *The faces of the Grassmannian of three-planes in* $\mathbf{R}^7$ *(calibrated geometries on* $\mathbf{R}^7$*)*, Invent. Math. **83** (1986), no. 2, 191–228.

[4] Frank Morgan, *The exterior algebra* $\Lambda^k\mathbf{R}^n$ *and area minimization*, Linear Algebra Appl. **66** (1985), 1–28.

[5] Raman Sanyal, Frank Sottile, and Bernd Sturmfels, *Orbitopes*, Mathematika **57** (2011), 275–314.

The Classification of compact Nil-manifolds up to isometry

Ulrich Brehm

Nil is one of the eight 3-dimensional Thurston geometries. We give a complete classification of all compact Nil-manifolds up to isometry. A compact Nil-manifold is by definition a compact 3-dimensional connected Riemannian manifold such that its universal cover is isometric to Nil. There is a canonical bijection between the isometry classes of compact Nil-manifolds and the conjugacy classes of cocompact fixed-point free discrete subgroups G of the isometry group Iso(Nil) of Nil. The isometry group of the Nil-manifold Nil$/G$ is isomorphic to $\mathrm{Nor}(G)/G$, where $\mathrm{Nor}(G)$ denotes the normalizer of G.

We use the linear model of Nil which has been introduced by K. Brodaczewska in her thesis [1]. In this model, Nil is $\mathbb{R}^3$ with the Riemannian metric $ds^2 = dx^2 + dy^2 + (\frac{y}{2}dx - \frac{x}{2}dy + dz)^2$. The isometry group Iso(Nil) is in this model a 4-dimensional subgroup of the group of affine transformations of $\mathbb{R}^3$. Nil has a natural filtration by parallels to the z-axis. The space of fibres is canonically isometric to the Euclidean plane. Iso(Nil) preserves the filtration and operates on the space of fibres as the full isometry group (of Euclidean motions).

Iso(Nil) contains the rotations R_ϕ around the z-axis, and the reflection ρ at the x-axis, and the Nil-translations $T_{(a,b,c)}$ with

$$T_{(a,b,c)} \begin{pmatrix} x \\ y \\ z \end{pmatrix} = \begin{pmatrix} x+a \\ y+b \\ z+c+\frac{1}{2}(ay-bx) \end{pmatrix}.$$

Each element of Iso(Nil) has a unique representation of the form $T_{(a,b,c)}R_\phi$ or $T_{(a,b,c)}R_\phi\rho$. Note that the group of Nil-translations operates simply transitive on Nil and that

$$T^{-1}_{(a,b,0)}T^{-1}_{(c,d,0)}T_{(a,b,0)}T_{(a,b,0)} = T_{(0,0,ad-bc)}.$$

We first consider the conjugacy classes of elements of Iso(Nil). Each element of Iso(Nil) is conjugate to exactly one of the following elements: The identity, a z-translation $T_{(0,0,u)}$ with $u > 0$, a Nil-translation $T_{(a,0,0)}$ with $a > 0$, a rotation R_ϕ with $\phi \in (0,\pi]$ around the z-axis, a screw $T_{(0,0,u)}R_\phi$ with $\phi \in (0,2\pi)$ and $u > 0$, the line reflection ρ, or a line glide reflection $T_{(a,0,0)}\rho$ with $a > 0$.

Let G be a cocompact fixed point free discrete subgroup of Iso(Nil). Let N denote the group of z-translations in G. Then G/N operates canonically on the space of fibres as a discrete cocompact group of Euclidean motions containing no reflections. Thus G/N is isomorphic to one of the seven crystallographic groups $p1, p2, p3, p4, p6, pg, pgg$.

A crucial observation for the classification of compact Nil manifolds is that each cocompact group of Nil-translations is conjugate to a group of the form

$$\langle T_{(a,0,0)}, T_{(b,c,0)}, T_{(0,0,\frac{ac}{k})}\rangle,$$

where $0 < a \leqslant c$ and $0 \leqslant b \leqslant \frac{a}{2}$ and $a^2 \leqslant b^2 + c^2$ and $k \in \mathbb{N}$. These a, b, c, k are uniquely determined by the conjugacy class. This is the classification in the case $p1$ and the basis for the classification in each of the other cases $p2, p3, p4, p6, pg$ and pgg.

Note that $T_{(0,0,ac)}$ is the commutator of $T_{(a,0,0)}$ and $T_{(b,c,0)}$. The number k is crucial for the topology of the Nil-manifold.

Table 1. Complete classification / summary

type	para- meters	fundamentalgroup and homology group	condition
p1	3	$\{S, T, U \mid S^{-1}T^{-1}ST = U^k,$ $SU = US, TU = UT\}$ $\mathbb{Z} \oplus \mathbb{Z} \oplus Z_k$	$k \in \mathbb{N}$
p2	3	$\{A_1, A_2, A_3 \mid A_1^2 = A_2^2 = A_3^2,$ $(A_1A_2A_3)^2 = A_1^{2(3+k)}\}$ $Z_2 \oplus Z_2 \oplus Z_{2k}$	$k \equiv 0 \pmod{2}$
p3	1	$\{B_1, B_2 \mid B_1^3 = B_2^{-3},\ (B_1B_2)^3 = B_1^{3k)}\}$ $\{B_1, B_2 \mid B_1^3 = B_2^3,\ (B_1B_2)^3 = B_1^{3(2\pm k)}\}$ two different types $Z_3 \oplus Z_{3k}$ in each case	$k \not\equiv 0 \pmod{3}$ $k \equiv 0 \pmod{3}$ $k \in \mathbb{N}$
p4	1	$\{A, C \mid C^4 = A^2, (AC^{-1})^4 = A^{2(1+k)}\}$ and a different type $\{A, C \mid C^4 = A^2, (AC^{-1})^4 = A^{2(1-k)}\}$ $Z_2 \oplus Z_{4k}$ in each case	$k \equiv 0 \pmod{2}$ $k \equiv 0 \pmod{4}$ $k \equiv 0 \pmod{2}$
p6	1	$\{A, B \mid B^3 = A^2,\ (BA)^6 = A^{2(5+k)}\}$ and a different type $\{A, B \mid B^3 = A^2,\ (BA)^6 = A^{2(5-k)}\}$ Z_{6k} in each case	$k \equiv 0 \pmod{6}$ or $k \equiv 2 \pmod{6}$ $k \equiv 0 \pmod{6}$ or $k \equiv 4 \pmod{6}$ $k \equiv 0 \pmod{2}$
pg	2	$\{P, S, U \mid SPS = PU^k, PU = U^{-1}P,$ $SU = US\}$ $\mathbb{Z} \oplus Z_2 \oplus Z_2$ $\mathbb{Z} \oplus Z_4$	$k \in \mathbb{N}$ $k \equiv 0 \pmod{2}$ $k \equiv 1 \pmod{2}$
pgg	2	$\{P, Q, U \mid (QP)^2 = (P^{-1}Q)^2 = U^k,$ $UPU = P,\ UQU = Q\}$ $Z_4 \oplus Z_4$	$k \equiv 1 \pmod{2}$ $k \equiv 1 \pmod{2}$

Some infinite sequences of Nil-manifolds have been investigated before (e.g. [2], [3]), but not systematically.

The same methods and ideas can be applied to get also a complete classification of Nil-orbifolds up to isometry, but this has is not yet been completed.

The present work is part of the joint research project on Nil geometry between TU Dresden and Budapest Univ. Techn. Econ.

References

[1] Katarzyna Brodaczewska, *Elementargeometrie in Nil*, PhD thesis, TU Dresden, (2014).

[2] Emil Molnár, *On projective models of Thurston geometries, some relevant notes on Nil orbifolds and manifolds*, Siberian Electronic Mathemetical Reports **7(0)** (2010), 491–498.

[3] Emil Molnár and Jeno Szirmai, *On Nil crystallography*, Symmetry: Culture and Science **17(1-2)** (2006), 55–74.

[4] Emil Molnár, *The projective interpretation of the eight 3-dimensional homogeneous geometries*, Beiträge zur Algebra und Geometrie **38(2)** (1997), 261–288.

[5] Peter Scott, *The geometries of 3-manifolds*, Bulletin of the London Mathematical Society **15(5)** (1983), 401–487.

Kac-Ward formula and discrete boundary value problems coming from the critical Ising and double-Ising models in 2D

Dmitry Chelkak

1. Kac-Ward formula

1.1. Ising model. We begin this talk, based on a joint work in progress with D. Cimasoni and A. Kassel [1], with a new proof of the Kac-Ward formula [6, 5, 8]

$$[\mathrm{Z}_{\mathrm{Ising}}(G,(x_e)_{e\in E(G)})]^2 = \pm\det[\mathrm{KW}(G,(x_e)_{e\in E(G)})] \tag{1}$$

for the partition function of the spin Ising model on a planar graph G. In fact, we work with the low-temperature representation of the model so that the spins $\sigma_f = \pm 1$ are assigned to *faces* of G and parameters $x_e = \exp[-2J_e]$ describe their nearest-neighbor interactions across edges $e \in E(G)$. The particularly important setup is simply connected discrete domains Ω drawn on some fixed (e.g., square or honeycomb) planar grid, with constant interactions $x_e = x$. In this setup one can always assume that the big 'outer' face of $G = \Omega$ carries the spin $+1$, which is equivalent to say that all the boundary grid cells σ_f, $f \in \partial\Omega$, carry the spin $+1$.

1.2. Double-Ising model. The important feature of our proof comparing to other known ones, besides its simplicity and minimal number of cancellations involved, is that it provides a way to analyze the so-called *double-Ising model* in discrete domains via solutions to some special discrete boundary value problems; see Section 2.2. The double-Ising model on Ω is obtained by superimposing two copies of the Ising model: each face of Ω is in one of the *four* states '1'='$++$', '2'='$+-$', '3'='$--$', '4'='$-+$', and the interactions across edges are given by x_e for pairs $1|2, 1|4, 2|3$ and $2|4$, and by x_e^2 for $1|3$ and $2|4$. Assigning the state '1'='$++$' to all boundary faces $f \in \partial\Omega$ of Ω, we can reformulate (1) as follows:

$$\mathrm{Z}^{++}_{\text{dbl-I}}(\Omega) = [\mathrm{Z}^{+}_{\mathrm{Ising}}(\Omega)]^2 = \pm\det[\mathrm{KW}(\Omega)]\,, \tag{2}$$

where superscripts denote boundary conditions and we omit $x_e = x$ in the notation.

Now let us split the boundary $\partial\Omega$ into two complementary arcs (ab), (ba), and impose the following boundary conditions: the states of faces along (ab) are either '1'='+ +' or '3'='− −', while the faces along (ba) are '2'='+ −' or '4'='− +'. We call these *Dobrushin boundary conditions* since they generate an interface (domain wall) from a to b which separates the phase '1 or 3' from '2 or 4'. It is worth noting that we do *not* specify the state of any particular boundary face neither on (ab) nor on (ba), and include the possible x^2 interactions between those into the partition function. Then the following generalization of (1) holds:

$$\mathrm{Z}^{13|24}_{\text{dbl-I}}(\Omega, a, b) = \pm\, [\mathrm{KW}(\Omega, a, b)]^{-1}_{a,b} \cdot \det[\mathrm{KW}(\Omega, a, b)]\,, \tag{3}$$

where the superscript '13|24' stands for Dobrushin boundary conditions described above and $\mathrm{KW}(\Omega, a, b)$ is a modified Kac-Ward matrix defined below.

1.3. The matrices $\mathrm{KW}(\Omega)$, $\mathrm{KW}(\Omega, a, b)$ and proofs of identities (1)–(3). The entries of Kac-Ward matrices are labeled by oriented edges of G, we denote this set by $\mathbb{E}(G)$. When working with discrete domains Ω, it is also convenient to include all 'normal to $\partial\Omega$' edges (i.e., those separating faces on the boundary of Ω) into $\mathbb{E}(\Omega)$. Then, for $e, e' \in \mathbb{E}(\Omega)$, we set $[\mathrm{KW}(\Omega)]_{e,e'} := 0$ except

$$[\mathrm{KW}(\Omega)]_{e,e'} := \begin{cases} 1, & \text{if } \bar{e}' = e, \\ -(x_e x_{e'})^{1/2} \cdot \exp[\tfrac{i}{2}\alpha(e, \bar{e}')], & \text{if } \bar{e}' \text{ prolongates } e \text{ and } e' \neq e, \end{cases}$$

where $\bar{e}'$ denotes e' with the orientation inverted and $\alpha(e, \bar{e}')$ is the turning angle from e to $\bar{e}'$. It is worth noting that the classical Kac-Ward matrix [6] slightly *differs* from the matrix $\mathrm{KW}(\Omega)$ defined above. Namely, the former can be obtained by multiplying the latter by the trivial matrix $[J]_{e,e'} = \delta_{e,\bar{e}'}$ with $\det J = \pm 1$.

Sketch of the proof of identity (2). We consider the so-called *terminal graph* $T(\Omega)$ whose vertices are in 1-to-1 correspondence with oriented edges of Ω. Note that $\mathrm{KW}(\Omega)$ is a weighted adjacency matrix of $T(\Omega)$ which has edges of two sorts: 'long' edges linking e with $\bar{e}$ and 'short' ones linking e with e', if $\bar{e}'$ prolongates e. Expanding $\det \mathrm{KW}(\Omega)$, one gets terms labeled by coverings of $T(\Omega)$ by oriented cycles and double-edges. It is easy to see that two opposite orientations of a cycle produce a cancellation for odd-length cycles and a factor 2 for even-length ones.

For simplicity, let us assume that Ω is a trivalent graph; see [1] for the general case. A covering of $T(\Omega)$ consisting of even cycles and double edges can be interpreted as a double-Ising model configuration (on faces of Ω) as follows: cycles correspond to interfaces separating '1 or 3' from '2 or 4', short double edges form interfaces 1|3 or 2|4, while long double edges mean no change of the states '1'–'4' across them. Moreover, the additional factors 2 per cycle exactly correspond to the remaining ambiguity of assigning the face states given all the interfaces. □

The modified Kac-Ward matrix $\mathrm{KW}(\Omega, a, b)$ is defined as

$$[\mathrm{KW}(\Omega, a, b)]_{e,e'} := \begin{cases} \mp i x_e, & \text{if } e = e' \text{ is 'outward normal' to } \partial\Omega,\ e \neq a, b, \\ [\mathrm{KW}(\Omega)]_{e,e'}, & \text{otherwise,} \end{cases}$$

where the sign is $-$ for 'outward normal' edges on (ab) and $+$ for those on (ba).

Sketch of the proof of identity (3). The proof goes along the same lines as above. Expanding the minor of $\mathrm{KW}(\Omega, a, b)$ labeled by $\mathbb{E}(\Omega)\setminus\{a, b\}$, one interprets all non-canceling terms (a path from a to b + even-length cycles + double-edges) as double-Ising configurations with Dobrushin boundary conditions. □

2. Boundary value problems and convergence for $x = x_{\mathrm{crit}}$

2.1. Ising model. It was noticed in [7] that, at the *critical temperature* $x = x_{\mathrm{crit}}$, the entries of $\mathrm{KW}(\Omega)^{-1}$ can be interpreted as discrete s-holomorphic functions [4] satisfying some special boundary conditions on $\partial\Omega$. In particular, let a, b be two 'outward normal to $\partial\Omega$' edges, and b be oriented horizontally to the right. Let

$$F_a(z_e) := [\mathrm{KW}(\Omega)]^{-1}_{a,e} + [\mathrm{KW}(\Omega)]^{-1}_{a,\bar{e}}\,,$$

where z_e denotes a midpoint of an edge in Ω and $e, \bar{e}$ stand for two possible orientations of this edge. Two crucial facts which eventually allow one to prove the convergence of interfaces in the critical Ising model to conformally invariant limits given by Schramm's SLE(3) curves are the following (see [2] for details):

- For each midedge z_e in Ω, the ratio $F_a(z_e)/F_a(z_b)$ is a martingale with respect to the interface (separating '–' and '+' states) running from a to b in the Ising model with Dobrushin boundary conditions ('–' on (ab), '+' on (ba)).
- The function $F_a(\cdot)/F_a(z_b)$ is s-holomorphic inside Ω. Moreover, for each 'outward normal to $\partial\Omega$' edge $c \neq a$, one has $\mathrm{Im}[F_a(z_c)/F_a(z_b) \cdot \sqrt{c}\,] = 0$, and this discrete boundary value problem determines the function $F_a(\cdot)$ uniquely.

Also, note that the analysis of similar boundary value problems and the convergence of their solutions to continuous counterparts are the core ingredients in a series of recent papers (see [2, 3] and references therein) devoted to the conformal invariance phenomenon in the critical 2D Ising model on bounded planar domains.

2.2. Double-Ising model with Dobrushin boundary conditions. Denote

$$F_{a,b}(z_e) := [\mathrm{KW}(\Omega, a, b)]^{-1}_{a,e} + [\mathrm{KW}(\Omega, a, b)]^{-1}_{a,\bar{e}}\,.$$

- Then, for each midedge z_e in Ω, the ratio $F_{a,b}(z_e)/F_{a,b}(z_b)$ is a martingale with respect to the interface (13|24 domain wall) running from a to b in the double Ising model with Dobrushin boundary conditions ('1 or 3' on (ab), '2 or 4' on (ba)).
- The function $F_{a,b}(\cdot)/F_{a,b}(z_b)$ is s-holomorphic inside Ω. Moreover, one has $\mathrm{Im}[F_{a,b}(z_c)/F_{a,b}(z_b) \cdot (1 \mp ix)\sqrt{c}\,] = 0$ for each 'outward normal' edge $c \neq a$, where the sign is $-$ on (ab) and $+$ on (ba). These properties determine $F_{a,b}(\cdot)$ uniquely.

2.3. Wilson's conjecture on double-Ising interfaces. In [9], D. Wilson conjectured that '13|24' domain walls at the critical temperature $x = x_{\mathrm{crit}}$ converge to Schramm's SLE(4) curves *with drifts* depending on boundary conditions. A striking part of the conjecture is that, even for Dobrushin boundary conditions, these scaling limits are *not* expected to satisfy the so-called domain Markov property despite their discrete precursors doing so. It means that solutions to discrete boundary value problems from Section 2.2 are somehow sensitive to 'boundary effects', on the contrary to the fact that their analogues from Section 2.1 are not. At the moment, we do not know how to analyze such a dependence using the language of discrete s-holomorphic functions, which seems to be a challenging problem.

References

[1] D. Chelkak, D. Cimasoni, A. Kassel, *Revisiting the combinatorics of the 2D Ising model*, Preprint 2015, in preparation.

[2] D. Chelkak, H. Duminil-Copin, C. Hongler, A. Kemppainen, S. Smirnov, *Convergence of Ising interfaces to Schramm's SLE curves*, C. R. Acad. Sci. Paris, Ser. I **352** (2014), 157–161.

[3] D. Chelkak, C. Hongler, K. Izyurov, *Conformal invariance of spin correlations in the planar Ising model*, Ann. Math. **181** (2015), no. 3, 1087–1138.

[4] D. Chelkak, S. Smirnov, *Universality in the 2D Ising model and conformal invariance of fermionic observables*, Invent. Math. **189** (2012), no. 3, 515–580.

[5] D. Cimasoni, *A generalized Kac-Ward formula*, J. Stat. Mech., page P07023, 2010.

[6] M. Kac, J. C. Ward, *A combinatorial solution of the two-dimensional Ising model*, Phys. Rev. **88** (1952), 1332–1337.

[7] M. Lis, *The fermionic observable in the Ising model and the inverse Kac-Ward operator*, Ann. Henri Poincaré **15** (2014), no. 10, 1945–1965.

[8] M. Lis, *A short proof of the Kac-Ward formula*, Preprint arXiv:1502.04322.

[9] D. B. Wilson, *XOR-Ising Loops and the Gaussian Free Field*, Preprint arXiv:1102.3782.

The Morse theory of Čech and Delaunay complexes

Ulrich Bauer

(joint work with Herbert Edelsbrunner)

Given a finite set of points in $\mathbb{R}^n$ and a radius parameter, we study the Čech, Delaunay–Čech, Delaunay (or alpha), and Wrap complexes in the light of generalized discrete Morse theory. Establishing the Čech and Delaunay complexes as sublevel sets of generalized discrete Morse functions, we prove relationships between the functions that imply that the four complexes are simple-homotopy equivalent. Our results have applications in topological data analysis and in the reconstruction of shapes from sampled data.

1. Background

1.1. **Discrete Morse theory.** Let K be a finite simplicial complex. Recall that an *interval* in the face relation of K is a subset of the form

$$[P, R] = \{Q \mid P \subseteq Q \subseteq R\}.$$

We call a partition V of K into intervals a *generalized discrete vector field*. Suppose now that there is a function $f\colon K \to \mathbb{R}$ that satisfies $f(P) \leqslant f(Q)$ whenever P is a face of Q with equality iff P and Q belong to a common interval in V. Then f is called a *generalized discrete Morse function* and V is its *generalized discrete gradient.* If an interval contains only one simplex, then we call the simplex a *critical simplex* and the value of the simplex a *critical value* of f. A generalized discrete gradient can encode a simplicial collapse.

Theorem 1 (Generalized Collapsing Theorem [1, 4])**.** *Let K be a simplicial complex with a generalized discrete gradient V, and let $K' \subseteq K$ be a subcomplex. If $K \backslash K'$ is a union of non-singular intervals in V, then K collapses to K'.*

1.2. **Čech and Delaunay complexes.** For $r \geqslant 0$, let $B_r(x) = \{y \in \mathbb{R}^n \mid d(x, y) \leqslant r\}$ be the closed ball of radius r centered at $x \in X$. The *Čech complex* of a finite set $X \subseteq \mathbb{R}^n$ for radius $r \geqslant 0$,

$$\mathrm{Cech}_r(X) = \Big\{ Q \subseteq X \mid \bigcap_{x \in Q} B_r(x) \neq \varnothing \Big\},$$

is isomorphic to the nerve of the collection of closed balls.

For a finite set $X \subseteq \mathbb{R}^n$ and a point $x \in \mathbb{R}^n$, the *Voronoi domain* of x with respect to X, and the *Voronoi ball* of x with respect to X for a radius $r \geqslant 0$ are, respectively,

$$\mathrm{Vor}(x, X) = \{y \in \mathbb{R}^n \mid d(y, x) \leqslant d(y, p) \text{ for all } p \in X\} \text{ and}$$
$$\mathrm{Vor}_r(x, X) = B_r(x) \cap \mathrm{Vor}(x, X).$$

The *Delaunay complex* of X for radius $r \geqslant 0$,

$$\mathrm{Del}_r(X) = \Big\{ Q \subseteq X \mid \bigcap_{x \in Q} \mathrm{Vor}_r(x, X) \neq \varnothing \Big\},$$

often also called alpha complex, is isomorphic to the nerve of the collection of Voronoi balls.

The *Delaunay–Čech complex* for radius $r \geqslant 0$ is the restriction of the Čech complex to the Delaunay triangulation. It contains all simplices in the Delaunay triangulation such that the balls of radius r centered at the vertices have a non-empty common intersection:

$$\mathrm{DelCech}_r(X) = \Big\{ Q \in \mathrm{Del}(X) \mid \bigcap_{x \in Q} B_r(x) \neq \varnothing \Big\}.$$

2. Selective Delaunay complexes and their discrete gradients

Generalizing the Čech and Delaunay complexes, the *selective Delaunay complex* of $E \subseteq X$ and r contains all simplices over X whose vertices have Voronoi balls for the subset E with non-empty common intersection:

$$\mathrm{Del}_r(X, E) = \Big\{ Q \subseteq X \mid \bigcap_{x \in Q} \mathrm{Vor}_r(x, E) \neq \varnothing \Big\}.$$

The Čech and Delaunay complexes appear as special cases $\mathrm{Cech}_r(X) = \mathrm{Del}_r(X, \varnothing)$ and $\mathrm{Del}_r(X) = \mathrm{Del}_r(X, X)$.

There is an equivalent definition of selective Delaunay complexes in terms of radius functions. We write $S(Q, E)$ for the smallest $(n-1)$-dimensional sphere S such that all points of Q lie on or inside S and all points of E lie on or outside S, if such a sphere exists, referring to it as the *Delaunay sphere* of Q for E, and we write $s(Q, E)$ for its squared radius. The *radius function* for E is defined by $s_E(Q) = s(Q, E)$. Now a subset $Q \subseteq X$ is a simplex in $\mathrm{Del}_r(X, E)$ iff $s_E(Q) \leqslant r^2$.

A finite set $X \in \mathbb{R}^n$ is in *general position* if every subset $Q \subseteq X$ of at most $n + 1$ points is affinely independent and no point of $X \backslash Q$ lies on the smallest circumsphere of Q.

Let S be an $(n-1)$-sphere, write $\mathrm{Incl}\, S, \mathrm{Excl}\, S \subseteq X$ for the subsets of included and excluded points, and set $\mathrm{On}\, S = \mathrm{Incl}\, S \cap \mathrm{Excl}\, S$. Assuming that S is the smallest circumsphere of $\mathrm{On}\, S$, we can write the center z as an affine combination $z = \sum \rho_x x$ of $\mathrm{On}\, S$. If X is in general position, the affine combination is unique, and $\rho_x \neq 0$ for all $x \in \mathrm{On}\, S$. We call

$$\mathrm{Front}\, S = \{x \in \mathrm{On}\, S \mid \rho_x > 0\},$$
$$\mathrm{Back}\, S = \{x \in \mathrm{On}\, S \mid \rho_x < 0\}$$

the *front face* and the *back face* of $\mathrm{On}\, S$, respectively. Using these definitions, we can state combinatorial conditions characterizing the Delaunay spheres. These conditions are derived from the *Karush–Kuhn–Tucker* conditions, using the observation that Delaunay spheres are defined as minimizers of a certain convex optimization problem.

Theorem 2 (Combinatorial KKT Conditions)**.** *Let X be a finite set of weighted points in general position. Let $Q, E \subseteq X$ for which there exists a sphere S with $Q \subseteq \mathrm{Incl}\, S$ and $E \subseteq \mathrm{Excl}\, S$. It is the smallest such sphere, $S = S(Q, E)$, iff*

(i) S is the smallest circumsphere of $\mathrm{On}\, S$,
(ii) $\mathrm{Front}\, S \subseteq Q$, and
(iii) $\mathrm{Back}\, S \subseteq E$.

Corollary 1 (Selective Delaunay Morse Function Corollary)**.** *Let X be a finite set of weighted points in general position, and $E \subseteq X$. Then the radius function*

$$s_E \colon \mathrm{Del}(X, E) \to \mathbb{R}$$

is a generalized discrete Morse function whose gradient consists of the intervals $[\mathrm{Front}\, S, \mathrm{Incl}\, S]$ over all Delaunay spheres $S = S(Q, E)$ with $Q \in \mathrm{Del}(X, E)$.

Corollary 2 (Critical Simplex Corollary)**.** *Let X be a finite set of weighted points in general position. Independent of E, a subset $Q \subseteq X$ is a critical simplex of s_E, with critical value $s(Q, Q)$, iff Q is a centered Delaunay simplex.*

3. Collapses

Given $E \subseteq F \subseteq X$, we can refine the generalized discrete gradients of the two radius functions s_E and s_F to a discrete gradient that induces a sequence of collapses.

Theorem 3. $\mathrm{Del}_r(X, E) \searrow \mathrm{Del}_r(X, E) \cap \mathrm{Del}(X, F) \searrow \mathrm{Del}_r(X, F)$.

In particular, we obtain a collapse of the Čech complex through the Delaunay–Čech complex to the Delaunay complex.

Corollary 3. $\mathrm{Cech}_r(X) \searrow \mathrm{DelCech}_r(X) \searrow \mathrm{Del}_r(X)$.

The face relation induces a partial order on the generalized gradient V_X of the Delaunay function s_X. The lower set of a subset $A \subseteq V_X$ in this partial order is denoted by $\downarrow A$. We can now give a very simple definition of the *Wrap complex* [3] for $r \geqslant 0$, consisting of all simplices in the lower sets of all singleton intervals with Delaunay sphere of radius at most r:

$$\mathrm{Sing}_r(X) = \{[Q,Q] \in V_X \mid s_X(Q) \leqslant r^2\},$$
$$\mathrm{Wrap}_r(X) = \bigcup \downarrow \mathrm{Sing}_r(X).$$

The Wrap complex is used in commercial software for surface reconstruction. The original definition of the Wrap complex corresponds to $\mathrm{Wrap}_\infty(X)$, which we simply denote as $\mathrm{Wrap}(X)$. The following collapse is immediate from the definition.

Theorem 4. $\mathrm{Del}_r(X) \searrow \mathrm{Wrap}(X)$.

References

[1] M. K. Chari, *On discrete Morse functions and combinatorial decompositions*, Discrete Mathematics **217** (2000), 101–113.

[2] H. Edelsbrunner, *The union of balls and its dual shape*, Discrete and Computational Geometry **13** (1995), 415–440.

[3] H. Edelsbrunner, *Surface reconstruction by wrapping finite sets in space*, Discrete and Computational Geometry: The Goodman-Pollack Festschrift, 379–404, Springer, 2003.

[4] R. Forman, *Morse theory for cell complexes*, Advances in Mathematics **134** (1998), 90–145.

Fixed-energy harmonic function

Richard Kenyon
(joint work with Aaron Abrams)

We study the map from conductances to edge energies for harmonic functions on graphs with Dirichlet boundary conditions. We prove that for any compatible acyclic orientation and choice of energies there is a unique choice of conductance such that the associated harmonic function realizes those orientations and energies. We call the associated function *enharmonic*. For rational energies and boundary data the Galois group of $\mathbb{Q}^{tr}$ (the totally real algebraic numbers) over $\mathbb{Q}$ permutes the enharmonic functions, acting (generically transitively) on the set of compatible acyclic orientations.

For planar graphs there is an enharmonic conjugate function; together these form the real and imaginary parts of a “fixed energy” analytic function, or *axilytic* function. In the planar scaling limit for $\mathbb{Z}^2$, these functions satisfy an analog of the Cauchy-Riemann equations, the axilytic equations

$$\begin{aligned} u_x v_y &= 1 \\ u_y v_x &= -1. \end{aligned}$$

We give an analog of the Riemann mapping theorem for injective axilytic functions, as well as a variational approach to finding solutions in both the discrete and continuous settings.

Open Problems in Discrete Differential Geometry

Collected by Günter Rote

PROBLEM 1 (Sergei Tabachnikov). Paper Möbius strip and paper cylinder eversion

One can make a smooth Möbius strip from a paper rectangle if its aspect ratio is sufficiently large, but not from a square.

Question 1. *What is the smallest length λ such that a smooth Möbius band can be made of a $1 \times a$ paper rectangle if $a > \lambda$?*

The known bounds are $\frac{\pi}{2} \leqslant \lambda \leqslant \sqrt{3}$ [1, 2], and it is conjectured that $\lambda = \sqrt{3}$. For smooth immersions, the answer is $\lambda = \pi/2$. See [3, 4, 5] and the references there for developable Möbius bands. A related problem concerns the eversion of a cylinder:

Question 2. *What is the least perimeter μ of a paper cylinder of height 1 that can be turned inside out in the class of embedded smooth developable surfaces.*

The known bounds are $\pi \leqslant \mu \leqslant \pi + 2$, and for smooth immersions, the answer is $\mu = \pi$ [2].

References

[1] D. Fuchs, S. Tabachnikov. *Mathematical omnibus. Thirty lectures on classic mathematics.* Amer. Math. Soc., Providence, RI, 2007.

[2] B. Halpern, C. Weaver. *Inverting a cylinder through isometric immersions and isometric embeddings.* Trans. Amer. Math. Soc. 230 (1977), 41–70.

[3] T. Randrup, P. Røgen. *Sides of the Möbius strip.* Arch. Math. 66 (1996), 511–521.

[4] I. Sabitov. *Isometric immersions and embeddings of a flat Möbius strip into Euclidean spaces.* Izv. Math. 71 (2007), 1049–1078.

[5] G. Schwarz. *The dark side of the Moebius strip.* Amer. Math. Monthly 97 (1990), 890–897.

PROBLEM 2 (Sergei Tabachnikov). Commuting billiard maps

Given a smooth convex plane domain, the billiard ball map sends an incoming ray (the trajectory of the billiard ball) that hits the boundary from inside to an outgoing ray according to the law of reflection: the angle of incidence equals the angle of reflection.

Consider two nested convex domains. The two billiard ball maps, T_1 and T_2, act on the oriented lines that intersect both domains. If the domains are bounded by confocal ellipses, then the respective billiard ball maps commute; see, e.g., [4].

Question. *Assume that the two maps commute: $T_1 \circ T_2 = T_2 \circ T_1$. Does it follow that the two domains are bounded by confocal ellipses?*

For piecewise analytic billiards, this conjecture was proved in [2]. For "outer billiards", an analogous fact is proved in [3]. Of course, this problem has a multi-dimensional version, open both for inner and outer billiards; see, e.g., [1] on multi-dimensional integrable billiards.

References

[1] V. Dragović, M. Radnović. *Poncelet porisms and beyond. Integrable billiards, hyperelliptic Jacobians and pencils of quadrics.* Birkhäuser, Basel, 2011.
[2] A. Glutsyuk. *On 4-reflective complex analytic planar billiards.* arXiv:1405.5990, 2014.
[3] S. Tabachnikov. *Commuting dual billiard maps.* Geom. Dedicata 53 (1994), 57–68.
[4] S. Tabachnikov. *Geometry and billiards.* Amer. Math. Soc., Providence, RI, 2005.

PROBLEM 3 (Mikhail Skopenkov). Inverse problem for alternating-current networks

An *alternating-current* network [2, Section 2.4] is a (not necessarily planar) graph with a fixed subset of b vertices (*boundary vertices*) and a complex number c_{xy} with positive real part (*conductance*) assigned to each edge xy. A *voltage* is a complex-valued function v_x on the set of vertices such that for each nonboundary vertex y we have $\sum_{xy} c_{xy}(v_x - v_y) = 0$, where the sum is over the edges containing the vertex y. One can see that the voltage is uniquely determined by its boundary values [2, Section 5.1]. The *current flowing into the network* through a boundary vertex y is $i(y) := \sum_{xy} c_{xy}(v_x - v_y)$. The network *response* is the matrix of the linear map taking the vector of voltages at the boundary vertices to the vector of currents flowing into the network through the boundary vertices.

The general *electrical-impedance tomography* problem is to reconstruct the network from its response. For direct-current planar networks, meaning that all conductances are real and positive, the problem has been solved [1].

Teaser. There is a matrix realizable as the response of the network in the figure to the right, for the boundary vertices N_1, N_2, N_3 and some edge conductances R_1, R_2, R_3, but not by the network to the left.

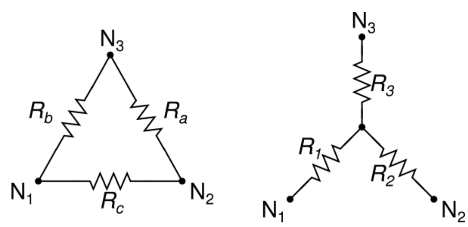

Denote by Ψ_b the set of complex $b \times b$ matrices Λ having the following 4 properties:

(1) Λ is symmetric;
(2) the sum of the entries of Λ in each row is zero;
(3) $\operatorname{Re}\Lambda$ is positive semidefinite;
(4) if $U = (U_1, \dots, U_b) \in \mathbb{R}^b$ and $U^T(\operatorname{Re}\Lambda)U = 0$ then $U_1 = \dots = U_b$.

Question 1. *Prove that the set of responses of all possible connected alternating-current networks with b boundary vertices is the set Ψ_b.*

It is known that Conditions (1–4) are necessary. Sufficiency is known for $b = 2$ and $b = 3$ [2, Theorem 4.7].

Question 2. *Provide an algorithm to reconstruct a network and edge conductances for a given response matrix.*

Note: Questions 1 and 2 have been solved by Günter Rote.

Question 3. *Describe the set of responses of all* series-parallel *networks.*

Question 4. *Describe the set of responses of all* planar *networks that have the boundary vertices on the outer face.*

Question 5. *Let the conductance of each edge be either ω or $1/\omega$, where ω is a variable. Describe the set of possible responses of such networks as functions in ω.*

This is known for $b = 2$ boundary vertices — Foster's reactance theorem [2, Theorem 2.5].

References

[1] E. B. Curtis, J. A. Morrow, *Inverse Problems for Electrical Networks*, Ser. Appl. Math., vol. 13, World Scientific, Singapore, 2000.

[2] M. Prasolov and M. Skopenkov, *Tiling by rectangles and alternating current*, J. Combin. Theory A 118:3 (2011), 920–937.

PROBLEM 4 (Nina Amenta). Are face angles determined by dihedral angles?

Stoker's conjecture says that, for a convex 3-polytope with given combinatorics, if all dihedral angles are specified (different from 0 and π), then all face angles are also determined.

Question. *Is this also true for a non-convex polytope?*

One may assume that the polytope is triangulated and that it is homeomorphic to a sphere.

PROBLEM 5 (Günter Rote). Existence of offset polytopes

We are given a non-convex three-dimensional polytope P whose boundary is homeomorphic to a sphere. We want to construct an *offset* polytope P_ε in which every face is translated outward by the same small distance ε. P_ε should not have other faces than the faces coming from P, and the boundary of P_ε should remain homeomorphic to a sphere. If P has a saddle-like vertex of degree 4 or larger, the result is not unique.

Question. *Does such an offset polytope always exist for sufficiently small $\varepsilon > 0$?*

It is enough to solve the problem locally for each vertex v of degree $d \geqslant 4$. Such a vertex will be blown up into $d - 2$ new vertices, connected by edges that form a tree. The faces of P_ε should be simply connected when clipped to a neighborhood of v.

PROBLEM 6 (Ulrich Bauer). Subdivision of discrete conformal structures

Let $\mathcal{T}$ be a triangulated surface, and let $\lambda, \mu\colon E_{\mathcal{T}} \to \mathbb{R}_{>0}$ be two discrete conformally equivalent metrics on $\mathcal{T}$, represented as edge lengths of the triangulation.

Here, discrete conformal equivalence means that the edge lengths of λ and μ for any edge ij between two vertices i, j are related by $\mu_{ij} = e^{\frac{1}{2}(u_i+u_j)}\lambda_{ij}$ for some function $u\colon V_{\mathcal{T}} \to \mathbb{R}$ on the vertices.

Question. *Is there a metric subdivision scheme that preserves the conformal equivalence?*

Specifically, a *subdivision* of a simplicial complex K is a complex K' such that $|K| = |K'|$ and each simplex of K' is contained in some simplex of K. A *metric subdivision scheme* is a map sending each simplicial complex K equipped with a metric λ to a subdivision K' of K equipped with a metric λ'. A particular example is the *barycentric subdivision.* The question is whether there exists a metric subdivision scheme such that the subdivided metrics λ' and μ' are still conformally equivalent.

References

[1] F. Luo. *Combinatorial Yamabe flow on surfaces.* Commun. Contemp. Math., 6(5):765–780, 2004.

PROBLEM 7 (Jim Propp, Richard Kenyon)**.** Disk packings of maximum area

Consider two disks of radius 1 with centers at $(\pm 1, 1)$. Together with the x-axis, they enclose at curved triangular region. Into this region, we want to place infinitely many non-overlapping disks that touch the x-axis, such that their total area is maximized.

Question. *Is it true that the greedy method of successively placing each new circle into the interstices such that they touch two previously placed circles will give the maximum area?*

PROBLEM 8 (Günter Rote)**.** A curious identity on self-stresses

Take the wheel graph G (the graph of a pyramid) embedded in the plane in general position, with a central vertex p_0 that is connected to vertices $p_1, \ldots, p_n$ $(n \geqslant 3)$ forming a cycle. On the $2n$ edges of this graph, we define the following function:

$$\omega_{i,i+1} := \frac{1}{[p_i p_{i+1} p_0][p_1 p_2 \ldots p_n]}, \qquad \omega_{0,i} := \frac{[p_{i-1} p_i p_{i+1}]}{[p_{i-1} p_i p_0][p_i p_{i+1} p_0][p_1 p_2 \ldots p_n]}.$$

for $i = 1, \ldots, n$, where $[q_1 q_2 \ldots q_k]$ denotes signed area of the polygon $q_1 q_2 \ldots q_k$, and $p_{n+1} = p_1$. This function is a *self-stress*: the equilibrium condition $\sum_j \omega_{ij}(p_j - p_i) = 0$ holds for every vertex i, where the summation is over all edges ij incident to i. Pick two arbitrary points a and b and define another function f_{ij} on the edges of G:

$$f_{ij} := [a p_i p_j][b p_j p_j],$$

Then we have the following identity, which was used (and proved) for $n = 3$ in [1].

$$\sum_{ij \in E(G)} \omega_{ij} f_{ij} = 1 \tag{1}$$

A different formula for f_{ij} that fulfills (1) is given by a line integral over the segment p_ip_j, see [1, Lemma 3.10]:

$$f'_{ij} := \tfrac{3}{2} \cdot \|p_i - p_j\| \cdot \int_{x=p_i}^{p_j} \|x\|^2 \, ds = \tfrac{1}{2} \cdot \|p_i - p_j\|^2 \cdot \left(\|p_i\|^2 + \|p_j\|^2 + \langle p_i, p_j \rangle\right)$$

Question 1. *Are there other graphs with n vertices and $2n-2$ edges, for which a self-stress ω satisfying* (1) *can be defined? The next candidates with* 6 *vertices are the graph of a triangular prism with an additional edge, and the complete bipartite graph $K_{3,3}$ with an additional edge.*

Question 2. *What is the meaning of the identity* (1)*? Is it an instance of a more general phenomenon? What are the connections to homology and cohomology?*

References

[1] Günter Rote, Francisco Santos, and Ileana Streinu, *Expansive motions and the polytope of pointed pseudo-triangulations*, in: Discrete and Computational Geometry—The Goodman-Pollack Festschrift, Springer, 2003, pp. 699–736, arXiv:math/0206027 [math.CO].

PROBLEM 9 (Hao Chen and Arnau Padrol, reported by Günter M. Ziegler)**.**
Approximately inscribed polytopes

Steinitz proved in 1928 [3] that not every combinatorial type of 3-polytope can be inscribed, that is, realized with all vertices on a sphere. However, a weak version of this is true: Due to the Koebe–Andreev–Thurston circle packing theorem (see e.g. [2, 4]), every 3-polytope can be realized with all edges tangent to the sphere – and thus it has a representation with

- all vertices outside a sphere
- all facets cutting into the sphere.

The question is whether this extends to higher dimensions:

Question. *Does every combinatorial type of d-polytope have a realization with*

- *vertices outside a $(d-1)$-sphere,*
- *facets cutting into the same $(d-1)$-sphere.*

Our conjecture is that this is false for $d > 3$, perhaps already for $d = 4$, but certainly for high dimensions d, where we know that there are infinitely many projectively unique polytopes. The examples constructed in [1] are essentially inscribable, but there should be other such polytopes whose "shape" is far off from that of a sphere/quadric. However, we have not been able to construct such a polytope yet.

References

[1] Karim Adiprasito and Günter M. Ziegler. *Many projectively unique polytopes.* Inventiones math., 199:581–652, 2015.

[2] Alexander I. Bobenko and Boris A. Springborn. *Variational principles for circle patterns, and Koebe's theorem.* Transactions Amer. Math. Soc., 356:659–689, 2004.

[3] Ernst Steinitz. *Über isoperimetrische Probleme bei konvexen Polyedern.* J. reine angewandte Math., 159:133–143, 1928.

[4] Günter M. Ziegler. *Convex polytopes: Extremal constructions and f-vector shapes.* In E. Miller, V. Reiner, and B. Sturmfels, editors, "Geometric Combinatorics", Proc. Park City Mathematical Institute (PCMI) 2004, pages 617–691, Providence, RI, 2007. Amer. Math. Society.

Reporter: Jan Techter

Participants

Dr. Arseniy Akopyan
Institute of Science & Technology
Austria
(IST Austria)
Am Campus 1
3400 Klosterneuburg
AUSTRIA

Prof. Dr. Nina Amenta
Department of Computer Science
University of California, Davis
One Shields Ave.
Davis, CA 95616-8633
UNITED STATES

Prof. Dr. Ulrich Bauer
Fakultät für Mathematik
Geometrie & Visualisierung (M10)
Technische Universität München
Boltzmannstraße 3
85747 Garching bei München
GERMANY

Prof. Dr. Mirela Ben-Chen
Computer Science Department
TECHNION
Israel Institute of Technology
Haifa 32000
ISRAEL

Prof. Dr. Alexander I. Bobenko
Institut für Mathematik
Fakultät II - Sekr. MA 8 - 3
Technische Universität Berlin
Straße des 17. Juni 136
10623 Berlin
GERMANY

Prof. Dr. Ulrich Brehm
Institut für Geometrie
Technische Universität Dresden
01062 Dresden
GERMANY

Dr. Ulrike Bücking
Institut für Mathematik
Fakultät II - Sekr. MA 8 - 3
Technische Universität Berlin
Straße des 17. Juni 136
10623 Berlin
GERMANY

Dr. Dmitry Chelkak
ETH - ITS Zürich
Clausiusstraße 47
8092 Zürich
SWITZERLAND

Prof. Dr. Adam Doliwa
Department of Mathematics &
Computer Sciences
University of Warmia & Mazury
ul. Sloneczna 54
10-710 Olsztyn
POLAND

Ekaterina Eremenko
Institut für Mathematik
Fakultät II - Sekr. MA 8 - 3
Technische Universität Berlin
Straße des 17. Juni 136
10623 Berlin
GERMANY

Prof. Dr. Vladimir V. Fock
Institut de Mathématiques
Université de Strasbourg
7, rue Rene Descartes
67084 Strasbourg Cedex
FRANCE

Dr. Felix Günther
Isaac Newton Institute for
Mathematical Sciences
Cambridge University
20 Clarkson Road
Cambridge CB3 OEH
UNITED KINGDOM

Prof. Dr. Tim Hoffmann
Zentrum Mathematik
Technische Universität München
Boltzmannstr. 3
85748 Garching b. München
GERMANY

Dr. Alec Jacobson
Department of Computer Science
Columbia University
500 West 120 Street
New York, NY 10027
UNITED STATES

Prof. Dr. Michael Kazhdan
Department of Computer Science
The John Hopkins University
229 Malone Hall
Baltimore, MD 21218
UNITED STATES

Prof. Dr. Richard Kenyon
Department of Mathematics
Brown University
Box 1917
Providence, RI 02912
UNITED STATES

Prof. Dr. Alastair D. King
Department of Mathematical Sciences
University of Bath
Claverton Down
Bath BA2 7AY
UNITED KINGDOM

Benno König
Zentrum Mathematik
Technische Universität München
Boltzmannstr. 3
85748 Garching b. München
GERMANY

Prof. Dr. Wolfgang Kühnel
Fachbereich Mathematik
Institut für Geometrie u. Topologie
Universität Stuttgart
70550 Stuttgart
GERMANY

Wai Yeung Lam
Institut für Mathematik
Fakultät II - Sekr. MA 8 - 1
Technische Universität Berlin
Straße des 17. Juni 136
10623 Berlin
GERMANY

Dr. Yaron Lipman
Department of Computer Science
and Applied Mathematics
The Weizmann Institute of Science
P.O.Box 26
Rehovot 76100
ISRAEL

Prof. Dr. Feng Luo
Department of Mathematics
Rutgers University
Hill Center, Busch Campus
110 Frelinghuysen Road
Piscataway, NJ 08854-8019
UNITED STATES

Dr. Christian Müller
Institut f. Diskrete Mathematik &
Geometrie
Technische Universität Wien
Wiedner Hauptstraße 8 - 10/104
1040 Wien
AUSTRIA

Dr. Fedor Nilov
Department of Geometry & Topology
Faculty of Mechanics & Mathematics
Moscow State University
Leninskie Gory
Moscow 119 992
RUSSIAN FEDERATION

Prof. Dr. Ulrich Pinkall
Institut für Mathematik
Technische Universität Berlin
Sekr. MA 8-1
Straße des 17. Juni 136
10623 Berlin
GERMANY

Prof. Dr. Konrad Polthier
Institut für Mathematik
Freie Universität Berlin
Arnimallee 6
14195 Berlin
GERMANY

Prof. Dr. Helmut Pottmann
Institut f. Diskr. Mathematik &
Geometrie
Technische Universität Wien
Wiedner Hauptstraße 8-10
1040 Wien
AUSTRIA

Sanjay Ramassamy
Department of Mathematics
Brown University
Box 1917
Providence, RI 02912
UNITED STATES

Olga Romaskevich
Mathématiques
École Normale Supérieure de Lyon
46, Allee d'Italie
69364 Lyon Cedex 07
FRANCE

Dr. Thilo Rörig
Institut für Mathematik, MA 8-3
Technische Universität Berlin
Straße des 17. Juni 136
10623 Berlin
GERMANY

Prof. Dr. Günter Rote
Institut für Informatik
Freie Universität Berlin
Takustr. 9
14195 Berlin
GERMANY

Andrew Sageman-Furnas
Institut f. Numerische & Angew.
Mathematik
Universität Göttingen
Lotzestr. 16-18
37083 Göttingen
GERMANY

Prof. Dr. Raman Sanyal
Institut für Mathematik
Freie Universität Berlin
Arnimallee 2
14195 Berlin
GERMANY

Prof. Dr. Wolfgang K. Schief
School of Mathematics & Statistics
The University of Sydney
Sydney NSW 2052
AUSTRALIA

Prof. Dr. Jean-Marc Schlenker
Mathematics Research Unit, FSTC
University of Luxembourg
Campus Kirchberg
1359 Luxembourg
LUXEMBOURG

Prof. Dr. Peter Schröder
Annenberg Center, CMS
MC 305-16
California Institute of Technology
1200 E. California Blvd.
Pasadena, CA 91125
UNITED STATES

Dr. Mikhail Skopenkov
National Research University
Higher School of Economics
Department of Mathematics
Vavilova 7
Moscow 117 332
RUSSIAN FEDERATION

Lara Skuppin
Institut für Mathematik
Fakultät II - Sekr. MA 8 - 3
Technische Universität Berlin
Straße des 17. Juni 136
10623 Berlin
GERMANY

Prof. Dr. Boris Springborn
Institut für Mathematik, MA 8 - 3
Technische Universität Berlin
Straße des 17. Juni 136
10623 Berlin
GERMANY

Prof. Dr. Kenneth Stephenson
Department of Mathematics
University of Tennessee
320 Ayres Hall
Knoxville, TN 37996-1300
UNITED STATES

Prof. Dr. John M. Sullivan
Institut für Mathematik
Technische Universität Berlin
Sekr. MA 8-1
Straße des 17. Juni 136
10623 Berlin
GERMANY

Prof. Dr. Yuri B. Suris
Fachbereich Mathematik
Sekr. MA 7-2
Technische Universität Berlin
Straße des 17. Juni 135
10623 Berlin
GERMANY

Prof. Dr. Sergei Tabachnikov
Department of Mathematics
Pennsylvania State University
University Park, PA 16802
UNITED STATES

Jan Techter
Institut für Mathematik
Fakultät II - Sekr. MA 8 - 3
Technische Universität Berlin
Straße des 17. Juni 136
10623 Berlin
GERMANY

Alexander Thumm
Fachbereich Mathematik
Institut für Geometrie und Topologie
Universität Stuttgart
70550 Stuttgart
GERMANY

Prof. Dr. Yiying Tong
Department of Computer Science &
Engineering
Michigan State University
428 S. Shaw Lane #3115
East Lansing, MI 48824
UNITED STATES

Prof. Dr. Etienne Vouga
Department of Computer Science
The University of Texas at Austin
2317 Speedway, Stop D 9500
Austin, TX 78712
UNITED STATES

Prof. Dr. Johannes Wallner
Institut für Geometrie
Technische Universität Graz
Kopernikusgasse 24
8010 Graz
AUSTRIA

Prof. Dr. Max Wardetzky
Institut f. Numerische & Angew.
Mathematik
Universität Göttingen
Lotzestr. 16-18
37083 Göttingen
GERMANY

Prof. Dr. Günter M. Ziegler
Institut für Mathematik
Freie Universität Berlin
Arnimallee 2
14195 Berlin
GERMANY

Prof. Dr. Denis Zorin
Vision, Learning and Graphics Group
Computer Science Department
Courant Institute of Mathematical
Sciences
New York University
719 Broadway, 12th Fl.
New York NY 10003
UNITED STATES